

[Reprinted from BULLETIN OF THE AMERICAN METEOROLOGICAL SOCIETY, Vol. 62, No. 2, February 1981]  
Printed in U. S. A.

**Stereographic Observations from  
Geosynchronous Satellites:  
An Important New Tool  
for the Atmospheric Sciences**

A. F. Hasler

# Stereographic Observations from Geosynchronous Satellites: An Important New Tool for the Atmospheric Sciences

A. F. Hasler

Laboratory for Atmospheric Sciences  
Goddard Space Flight Center/NASA  
Greenbelt, Md. 20771

## Abstract

The capability of making stereographic observations of clouds and their temporal changes from two simultaneously scanning geosynchronous satellites is a new basic meteorological analysis tool with a broad spectrum of applications. Stereo height measurements, because of their higher horizontal resolution and dependence on only straightforward geometric relationships, represent a big improvement over previously used infrared-based techniques. Verification using high altitude mountain lakes indicates that stereo cloud height accuracies of  $\pm 0.1$ - $0.2$  km are possible near reference points of known elevation. The smallest cloud features observed by the present operational geosynchronous satellites (GOES), which have spatial and temporal resolution of 1.0 km and 3 min, can be measured with height accuracies of  $\pm 0.5$  km. Absolute stereo height accuracy, far from landmarks, is also about  $\pm 0.5$  km if accurate navigation solutions are available for both satellites. Computer remapping of digital image pairs allows the display and height measurement on time sequences of stereo images using an interactive information processing system. Rapid time sequencing of the series of stereo image pairs gives an effective 4-dimensional representation of cloud dynamics. Several interactive techniques have been developed for point measurements of cloud height and cloud height contouring. The stereo observations have been applied to meteorological problems, including: cloud top height contours of intense convective clouds in hurricanes and severe thunderstorms; cloud top and cloud base height estimates for satellite cloud-wind altitude assignment; atmospheric temperature profiles from the combination of stereo heights and infrared cloud top temperatures; determination of cloud emissivity; and finally, comparisons are made between stereo-observed, tropopause-penetrating thunderstorm tops with altitudes up to 17 km and severe weather observations from radar and surface reports. Present stereo coverage using the operational GOES satellites for research demonstrations includes large areas of North and South America and the surrounding oceans. Recommendations are given for operational stereo observations with greater coverage and improved performance employing a third GOES satellite at  $105^\circ\text{W}$ .

## 1. Introduction

The capability to make observations of clouds and their changes with time from geosynchronous satellite stereography is an important new basic meteorological analysis tool. These observations have much wider spatial coverage than previous stereography from ground, aircraft, and low-orbiting satellite platforms and better temporal resolution than is possible from proposed low-orbiting stereo satellites. It will be shown that stereo cloud height measurements from geosynchronous satellites can be made with high precision

and that the stereo height measurements can be made with much higher confidence than heights estimated from infrared-based techniques.

Remapping, display, and analysis of stereo images on an interactive computer/imaging system allows effective qualitative and quantitative representation of atmospheric dynamics. The value of the stereo observations is demonstrated by application to several meteorological problems. Recommendations for future improvements in stereo observations are also given.

### a. History of cloud stereography

Stereographic observations of the atmosphere, primarily photogrammetry of clouds from twin ground-based cameras or from time sequences of aerial photographs, have a long history. The first reference to aerial stereography in the literature is by Schereschewsky (1921), who used a side-looking camera. Descriptions of clouds and cloud regimes using this type of stereo data have been widely used by Malkus and Riehl (1964), Warner *et al.* (1979, 1980), and others. Undoubtedly, there was earlier work with ground-based cameras, but the first quantitative work on record is by Meyer (1954) and Kassander and Sims (1957).

Stereographic observations most similar to those from satellites are made from high-flying aircraft with a vertically-looking camera. An outstanding example of stereo photogrammetric analysis of this kind was made of severe thunderstorms by Roach (1967) using U-2 aircraft flying at an altitude of about 20 km.

Stereographic cloud observations from satellites were made by Ondrejka and Conover (1966) and Kikuchi and Kasai (1968) using early meteorological satellites equipped with vidicon tube cameras. Scanning radiometer systems on present operational meteorological satellites preclude stereography, although Lorenz and Schmidt (1979) propose a dual radiometer stereo system for future low-orbiting satellites. In 1968, high resolution stereo cloud photographs were taken from Apollo 6 in low earth orbit. Whitehead *et al.* (1969) and Shenk and Holub (1971) used these data to demonstrate the feasibility of making stereographic cloud height measurements. Then Shenk *et al.* (1975) analyzed a sequence of the Apollo 6 images to study the cloud structure associated with a strong cold front. More recently, Black (1977) has reported on stereo observations of hurricanes from Skylab. Unfortunately, stereography from low-orbiting satellites is not routinely available.

In 1974, the first operational geosynchronous satellite with the capability to produce high resolution (0.9 km) visible images (SMS-1) was launched and stationed at 75°W. With the successful operation of a second satellite (SMS-2 at 107°W) in February 1975, scientists from the Goddard Space Flight Center (GSFC) arranged a test of the stereo concept.<sup>1</sup> Scan-synchronized stereo image pairs were taken at the normal 30 min operational frequency.

The resulting hard copy images were analyzed using a modification to standard aerial stereo photogrammetric techniques (Minzer *et al.*, 1976, 1978). Point measurements of cloud height with accuracies of  $\pm 0.2$ – $0.5$  km and maps of cloud height with contours at 5 km intervals obtained from this work demonstrated the feasibility of stereo measurements. Independently, Bristor and Pichel (1974) had proposed the use of the two planned operational geosynchronous satellites (SMS-1 and SMS-2) for stereography and made a qualitative demonstration using images from the SMS-1 and ATS-3 satellites.

Work by Bryson (1978) with digital remapping of the GSFC's stereo SMS images confirmed the feasibility of making cloud height measurements. Independently, work had begun at GSFC on the digital remapping of the SMS images on the Atmospheric and Oceanographic Information Processing System (AOIPS) (desJardins, 1978)<sup>2,3</sup> for improved stereo display and height measurements. Interactive parallax measuring techniques and height calculation algorithms were developed and applied by Hasler *et al.* (1979a).<sup>2</sup>

On 26 May 1978, Goddard scientists arranged with NOAA to conduct the first operational scan synchronization of GOES East (75°W) and GOES West (135°W) for the purpose of *in situ* verification of stereo cloud heights. These data were used to conduct a stereo height verification experiment using high altitude mountain lakes as reported by Hasler *et al.* (1979a) and in this paper.

During the spring of 1979 the first scan synchronization of short interval (3 min) GOES images was performed for several days during SESAME '79 for the observation of severe thunderstorms. Radar, aircraft, and special network observations, as well as stereo satellite observations, were coordinated by SESAME '79 (Alberty *et al.*, 1979). The first scan synchronization of short interval images (7.5 min) for stereo observations of tropical cyclones was made on 12 September 1979 as Hurricane Frederic was approaching the Gulf Coast near Mobile, Ala.

#### b. Advantages of stereo over infrared techniques for the observations of cloud structure

Stereo measurements depend only on basic geometric relationships of observations of visible cloud particles, while in-

frared cloud top heights are dependent on knowledge of cloud emissivity, ambient temperature, and lapse rate; and also require the assumption that the cloud is in local thermodynamic equilibrium. In many important cases cloud emissivity and the atmospheric temperature height profile are unknown and the cloud is not in equilibrium with its environment.

The nominal spatial resolution of GOES visible images used for stereo is 0.9 km, vs. 8 km for the infrared. The infrared images are further degraded by slow sensor response (Negri *et al.*, 1976). Stereo observations have a vertical resolution approaching 0.1 km for large, high-contrast features, while for small features just resolved by the visible sensor (0.9 km) stereo height accuracy of only  $\sim 0.5$  km is possible (see Hasler *et al.*, 1979a; and Section 3b of this paper). On the other hand, the theoretical limit for infrared cloud height accuracy using GOES satellites is about 0.3 km, while errors of 1–2 km or greater are likely if any of the necessary assumptions are not valid.

#### c. Temporal and spatial coverage

Effective spatial coverage for the present GOES operational satellites at 75°W and 135°W incorporates a large area common to the two satellites, inclusive of most of the continental United States, but exclusive of the northeastern United States (see area enclosed by dashed line in Fig. 1, which is taken from Minzner *et al.* (1979)). Placement of a third satellite at about 105°W, similar to the location during the first stereo test in 1975, would give improved coverage and performance for the entire continental United States (see total hatched area in Fig. 1). Present temporal coverage is restricted to daylight hours. The coverage could be extended to nighttime hours using higher resolution infrared observations (Hasler *et al.*, 1979a) or visible sensors with enough sensitivity to observe clouds at night by moonlight.

Clouds of primarily vertical orientation or with extensive anvils will have their sides as well as base areas hidden from view (see Fig. 2), and this effect is greater with the large longitudinal separation (60°) of the present satellites. A third satellite at 105°W would reduce this problem by decreasing the maximum separation between satellite pairs to 30°.

## 2. Techniques

#### a. Background

Stereo height measurements require angular measurements of the target from the two satellites, given the relative positions of the two satellites and the earth. A simplified 2-dimensional diagram (see Fig. 3) shows how a cloud near sea level ( $C_0$ ), at a low elevation ( $C_h$ ), and at a greater elevation ( $C_H$ ) would be observed by the two satellites. Only  $C_0$  appears at its true location on the earth. The rays passing from GOES East and GOES West through  $C_h$  and  $C_H$  intersect the earth at points that increase in separation with increasing cloud height ( $C_hE - C_hW$ ,  $C_H E - C_H W$ ).

With accurate knowledge of the position of the two satellites relative to the earth at the time of observation (satellite ephemeris or orbit data) and the points where the rays intersect the earth from the image navigation, the height of the

<sup>1</sup> Private communication from W. E. Shenk to R. Wirth, 12 December 1974.

<sup>2</sup> All software packages used for digital stereo remapping and interactive stereo display and analysis on AOIPS were written by M. desJardins.

<sup>3</sup> For information on AOIPS see: Bracken, P. A., J. T. Dalton, J. B. Billingsley, and J. J. Quann, 1977: Atmospheric and Oceanographic Information Processing System (AOIPS) system description. March 1977. NASA/GSFC X-933-77-148.

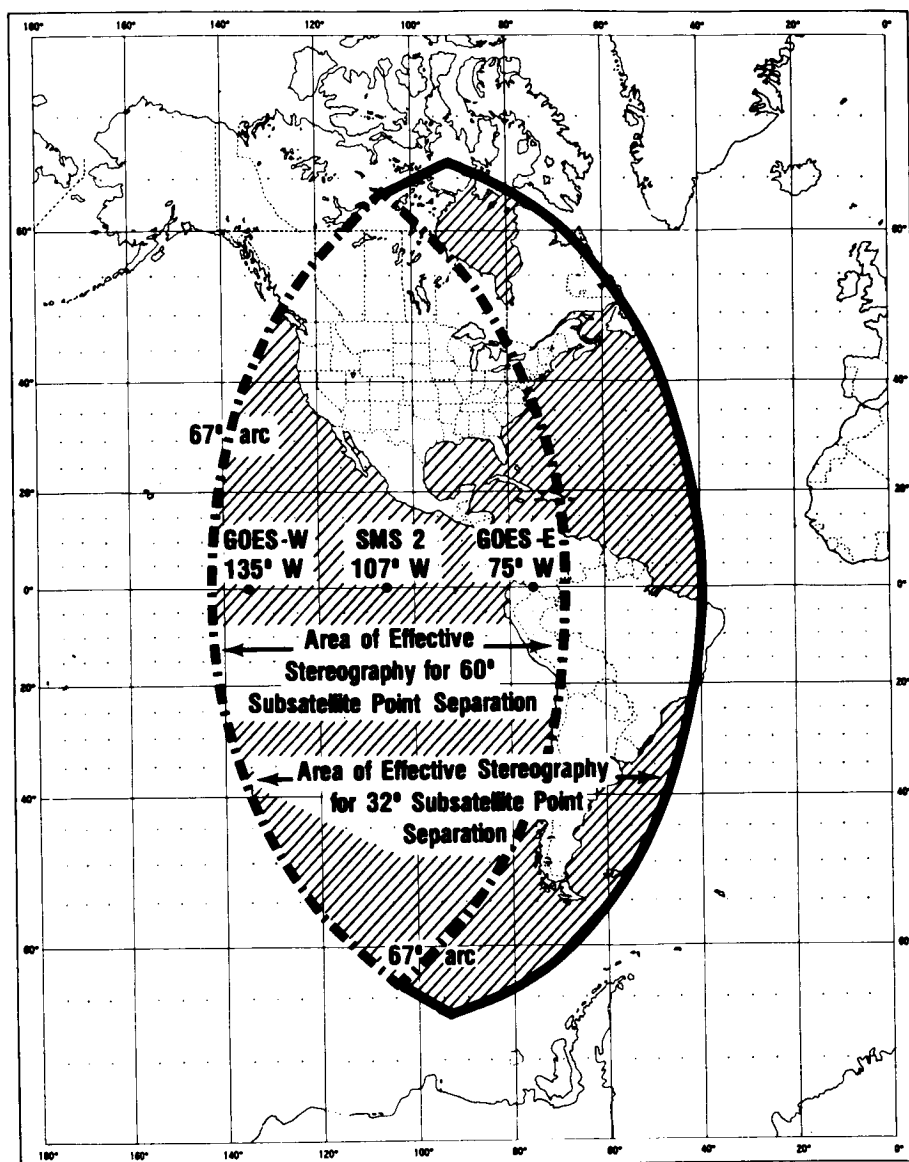


FIG. 1. Mercator projection map of the Western Hemisphere, showing the effective stereo coverage of geosynchronous satellites separated by 30° and 60° of longitude (from Minzner *et al.*, 1979). Accurate stereo height measurements may be made within the area enclosed by the dashed lines, given the present separation of the operational GOES satellites of 60°. If an additional satellite were moved to the location formerly occupied by SMS-2 at 107°W, coverage and performance would be dramatically improved (see total hatched area).

cloud ( $h$  or  $H$ ) can be obtained using spherical trigonometry.

For special cases over very limited areas it is possible to see the clouds stereoscopically using hard copy images in a standard stereo viewing apparatus. However, the wide separation of the two satellites and the curvature of the earth make it necessary to remap the images from one satellite into the coordinate system of the other for optimum viewing and height measurement. With computer remapping of digital images, stereo time sequences can be displayed that give great insight into atmospheric dynamics and from which precise quantitative measurements of cloud geometry can be made.

#### b. Remapping

Minzner *et al.* (1978) used a biaxial-tilting-table stereo viewing device that performed a limited remapping on hard copy images.

The computer remapping procedure used in this work is performed on digital images (Dalton *et al.*, 1979). The first step in the remapping is to do the best possible navigations of the images from both satellites. Navigation is done on AOIPS by combining orbit data with landmarks measured using interactive image alignment (Chen, 1980). The result is an algorithm that computes image coordinates (line, pixel)

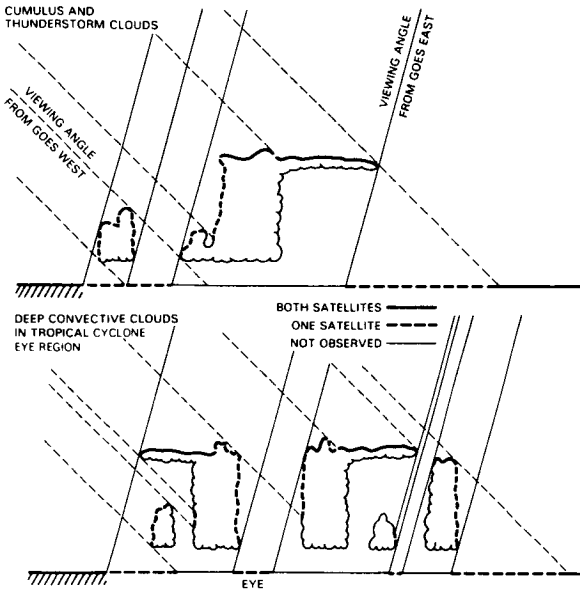


FIG. 2. Schematic cross section of typical storm clouds, illustrating the cloud surfaces that are observed in stereo and the gaps in the coverage for geosynchronous satellites that are separated by 60° of longitude. Cloud surfaces with large vertical extent are not observed by both satellites.

given earth coordinates (latitude, longitude), and vice versa. Knowledge of the earth coordinates for the images from both satellites allows them to be linked together.

Remapping is performed on a large computer using bilinear transformation on a gridded output space (Dalton *et al.*, 1979). A bilinear resampling technique is routinely used, but nearest neighbor or cubic convolution options are available. Remapping of a 512 × 512 pixel image array requires 10 s of CPU time on an IBM 360-91 computer. Estimated remapping time on a minicomputer such as AOIPS would be 2 min, but for smaller arrays such as 128 × 128 pixels only 15 s is required.

Figure 3 also shows a simplified 2-dimensional representation of how the remapping works. Sea level features ( $C_0$ ) appear at the same location in unremapped and remapped images ( $C_{0E}$ ,  $C_{0WR}$ ), while features above sea level ( $C_h$ ,  $C_H$ ) are displaced in an amount proportional to the height of the two images ( $C_{hE} - C_{hWR}$ ,  $C_{HE} - C_{HWR}$ ). This parallax gives the stereoscopic impression when the images are displayed.

c. Display

In order to obtain the highest quality images for stereo viewing the following image preprocessing functions are performed as required: 1) destriping (correction for nonlinear

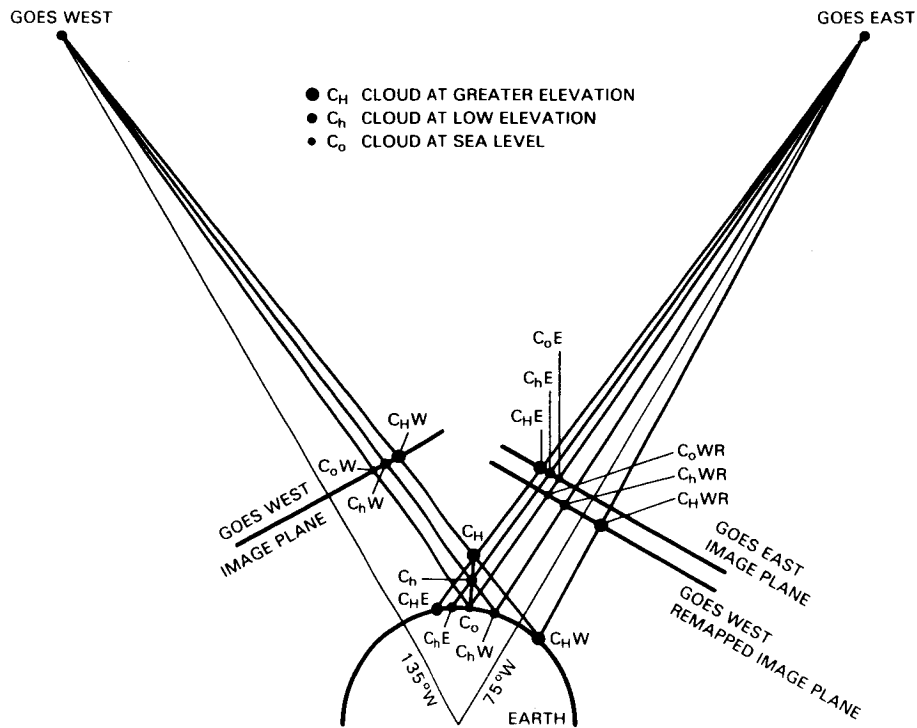


FIG. 3. Simplified 2-dimensional diagram illustrating how cloud height is observed by the two satellites. Remapping of the image of one satellite into the coordinate system of the other satellite is also shown. When the GOES East image is superimposed on the remapped GOES West image, sea level features ( $C_0$ ) should line up. The separation (parallax) between the two different images of the same cloud ( $C_{hE} - C_{hWR}$ ,  $C_{HE} - C_{HWR}$ ) is proportional to its height.

sensor response); 2) brightness normalization<sup>4</sup>; 3) image brightness enhancement; 4) interpolated image enlargement; and 5) edge enhancement. The standard stereo display on AOIPS involves projecting the unremapped (generally GOES East) image through the red gun of the television monitor and the remapped image (generally GOES West) through the blue and green guns. The resulting stereo pair is viewed through optical quality red and blue/green glasses or through red/green glasses with high quality celluloid filters. Rapid time sequencing of up to five stereo pairs is possible on the AOIPS, giving an effective 4-dimensional view of cloud dynamics. The red/green glasses give a separation of the images that is good enough for most purposes, but if 100% image separation is desired or if stereo color graphics are to be displayed, a split screen technique has also been developed that uses a prismatic hood for viewing. Electronically shuttered glasses have also been tested, but for most stereo the red/green glasses are the currently preferred viewing technique.

Another stereo viewing method that has also been found to be useful is a technique for making artificial stereo images from combining visible and infrared images (Pichel *et al.*, 1973). The technique produces a striking stereoscopic view that is of higher visual quality than the true stereo because all image features are seen with both eyes from the same viewing perspective. This technique is not very useful quantitatively, however, because heights are dependent on cloud emissivity and the IR resolution, and thus the heights often have large errors. The technique has the advantage of requiring much less data processing than the true stereo and it can be done with data from only one satellite. It has been found to be helpful in separating clouds at different levels and is particularly good for tracking cirrus.

#### d. Height measurement

Height measurement can be divided into two distinctly separate operations: 1) parallax measurements and 2) height calculations (desJardins, 1978). There are many techniques for parallax measurement. The object is to measure the location of a feature on each of the images of the stereo pair. In principle it is possible to locate a feature in two separate unremapped images, but this is possible only for very distinctive features and cannot be done with precision. Remapping of one image makes the shape of features viewed by both satellites appear more alike and is critical for accurate matching of features. Three different methods have been developed to increase the precision of parallax measurements and increase the number of features. The first method uses the red/green stereo glasses and the standard cursor on AOIPS. It also requires the AOIPS joystick controlled interactive image-shift capability. If one of the images of the stereo pair is shifted until the parallax for a feature is eliminated, the cursor appears at the height of the feature. The number of pixels the image was shifted to eliminate the parallax is then passed to the height calculation algorithm.

In the second method, stereo glasses are used only to give a qualitative impression of relative heights. The parallax is measured using an image alternation technique. It has been

determined that alternating images at varying rates is a very powerful method for detecting differences and for the determination of null motion points between images. This technique is also used by astronomers in their "blink comparators" and on AOIPS for the landmark measurements for navigation of GOES satellite images. In the image alternation technique, one of the images is shifted using the joystick until the motion of a feature is nulled. This technique is used for all quantitative parallax measurements not suitable for the third method.

The third method involves using a cross-correlation algorithm to eliminate the parallax between the two images of the stereo pair of a feature chosen by the operator. This objective technique, which can measure to subpixel accuracy, works best on large, well-defined, isolated features.

Once the parallax or image shift is determined by one of the three methods, the result is passed to the height calculation algorithm. An iterative technique is used to estimate the height of a feature (desJardins, 1978). First, the image shift (parallax) is used to compute the location of the feature on the original unremapped image. Then, by starting with an arbitrary height, the theoretical location of the cloud on the earth can be computed for each satellite. The height is then varied until the distance between the theoretical earth locations for the two satellites is minimized.

#### e. Cloud motion and height measurement

Software routines have been developed on AOIPS that allow interactive horizontal cloud motion measurement with the drawing of stereo marker arrows.<sup>5</sup> Stereo cloud-wind fields have also been measured using standard AOIPS single satellite techniques while referring frequently to stereo display and height measuring techniques for the separation of cloud tracer levels and for height assignment of the resulting winds.

#### f. Height contouring

Two manual height contouring techniques have been used to date. The first involves systematically measuring cloud heights on a grid and contouring the results manually. The second employs the image alternation technique. At any given image shift (parallax) cloud features with that shift will appear stationary, while features with greater or lesser shift will appear to move in opposite directions. Isoleths of constant shift can then be drawn and the height calculation algorithm used to convert these into true height contours.

### 3. Error analysis

#### a. Theoretical

Given perfect parallax measurement, the height measurement will still have the following sources of error: 1) refraction of light by the atmosphere, which has been neglected as an insignificant effect in both the navigation model and the height calculation; 2) errors introduced by geometric irregularities in the images caused by line jitter, nutation of the sat-

<sup>4</sup> Brightness normalization refers to the matching of the brightness of the two images in the stereo pair using the histogram techniques.

<sup>5</sup> For information on AOIPS see: Bracken, P. A., J. T. Dalton, J. B. Billingsley, and J. J. Quann, 1977: Atmospheric and Oceanographic Information Processing System (AOIPS) system description. March 1977, NASA/GSFC X-933-77-148.

ellite, etc.; 3) errors in the navigation solutions of the two satellites (due to landmarking errors, ephemeris errors, or errors in the navigation model), which will appear in both the remapping and in the height calculation; 4) heights computed relative to the earth surface as given by the oblate spheroid earth model used in the navigation model (desJardins, 1978); 5) nonlinearity of the images, which contributes to the error budget because of the bilinear interpolation that is used in the remapping process (desJardins, 1978); and 6) the bilinear resampling technique used in the remapping (desJardins, 1978).

Parallax measurements have errors due to two sources: 1) misidentification of the feature in the two images caused by differences in viewing angle, relative sun angle, sensor response, or image geometry irregularities; and 2) superposition errors due to granularity of the images, operator errors, or the lack of precision of the cross correlation of a given feature.

For nonstationary features (e.g., cloud features), errors in synchronization of the images also must be considered. Minzner *et al.* (1979) calculated that errors of less than 100 m in height would be introduced for clouds with speeds less than  $33 \text{ m s}^{-1}$  for scan synchronization within 4 s. The synchronization errors for most cases examined to date have been small. For example, during SESAME the error averaged 5 s for the severe thunderstorm observations on 2 and 3 May 1979, while the average scan synchronization error was 12 s for Hurricane Frederic on 12 September 1979. For larger time differences between the images of the stereo pair, corrections can be made by measuring the horizontal cloud motion from an image time sequence using one of the satellites. However, one must make two assumptions: 1) that the feature is still recognizable, and 2) that there is no significant vertical motion. For example, given a hypothetical synchronization error of about 30 s for the stereo images of severe thunderstorms in Oklahoma on 2 May 1979, a height error of 0.4 km would be caused by the  $25 \text{ m s}^{-1}$  easterly motion at cloud top. This error could then be removed with the limitations discussed previously.

Errors from any of the sources listed previously could have detrimental effects on the iterative height calculations. Errors will result if the measured parallax is not in the same direction as the theoretical parallax (desJardins, 1978). In the theoretical case, rays passing from the satellites to the earth intersect at the feature for which the height is desired. In

practice, because of the various errors, only the closest point of intersection can be determined. In the iterative scheme this problem is apparent when the distance between the calculated locations of the feature on the surface of the earth that is being minimized remains large. This value is used as a quality control criterion on AOIPS.

Minzner *et al.* (1979) have made estimates of the theoretical height errors for GOES satellites with various longitude separations. Minzner shows that as the longitude separation increases the height error for an ideal target decreases. For example, for the  $32^\circ$  and  $60^\circ$  longitude separations tested to date, the height error would be 0.5 and 0.25 km, respectively. In practice, however, large longitudinal separations require using data near the limb of one or both satellite images. Near the limb the horizontal resolution decreases so that the error in the position measurement of common features increases. A compromise between best stereo height resolution and best horizontal resolution will have to be determined so that the optimum longitude separation of the two satellites may be chosen.

*b. Empirical verification*

The maximum accuracy of satellite stereo cloud heights can be estimated by comparing the measurements of high altitude geographical features with topographical maps. Lakes with altitudes of up to 4 km provide the largest high contrast features, while mountains have altitudes up to  $\sim 6$  km in the Western Hemisphere if recognizable features can be found. Minzner *et al.* (1978) have measured both mountain and lake heights from satellites with a  $32^\circ$  longitude separation. They found for 16 mountain features and a lake that the stereo heights measured from hard copy images averaged 0.24 km higher than the corresponding map altitudes for those points with a standard deviation of 0.36 km.

Hasler *et al.* (1979a) performed an improved verification using a cross-correlation technique with subpixel accuracy on digitally remapped images of Lake Titicaca and several high altitude mountain lakes in the western United States with a satellite longitude separation of  $60^\circ$ . With nearby coastlines used as reference points and by comparison to topographic map altitudes, the stereo heights average 0.11 km lower with a standard deviation of 0.11 km.

Table 1 shows the results of an extension of this verification experiment. Only long high-contrast lakeshores or-

TABLE 1. Empirical stereo height ( $z$ ) verification from geosynchronous satellites at  $75^\circ\text{W}$  (GOES East) and  $135^\circ\text{W}$  (GOES West) with use of high altitude mountain lakes.

	Altitude (km)			
	$z_{\text{map}}$	$z$	$\sigma_z$	$z_{\text{map}} - z = \Delta z$
<i>I. Bias error estimates using coastlines</i>				
Baja, South America, California (9 sample areas)	0	0.09	0.31	-0.09
<i>II. Lake height comparison</i>				
California Lake Tahoe area				
Walker Lake	1.21	1.26	0.35	-0.05
Pyramid Lake	1.16	1.23	0.23	-0.07
Mono Lake	1.95	1.73	0.15	+0.22
South America Lake Titicaca area				
Lake Titicaca	3.82	3.68	0.18	+0.14
				$\overline{\Delta z} = 0.06, \sigma_{\Delta z} = 0.14$

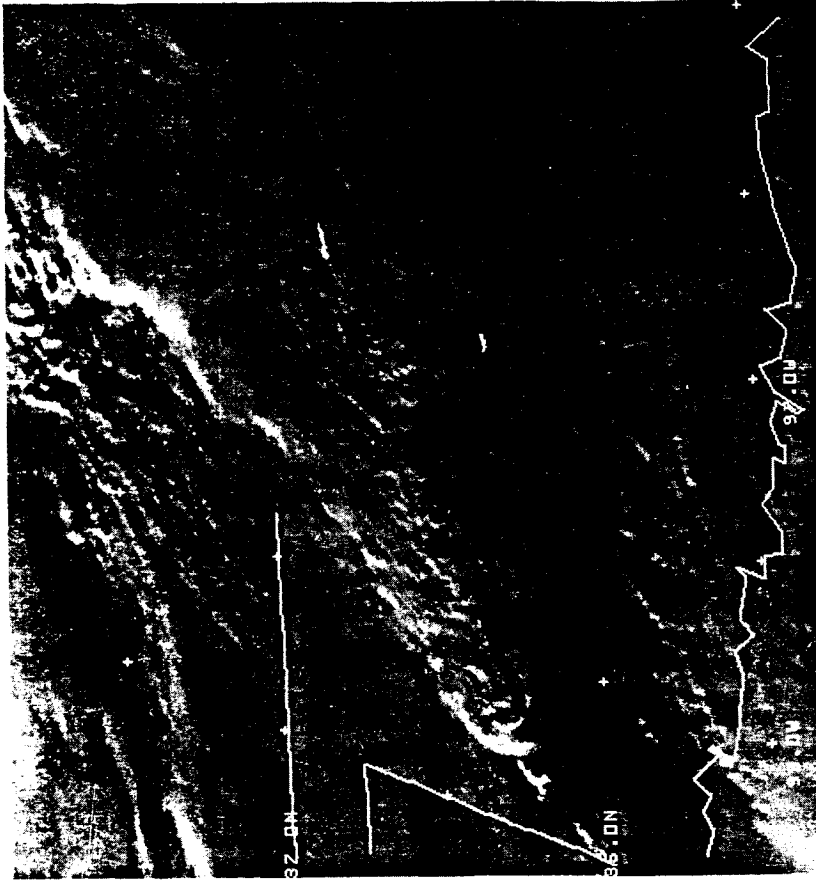


FIG. 5. GOES East image where the satellite scanned the same storm as in Fig. 4 at 0051:27 GMT. The synchronization error between the two images is 8 s. Figures 4 and 5 may be viewed stereoscopically by using a stereoscopic viewer or by observing the cover photo with the red/green (anaglyph) glasses inserted between cover 2 and p. 193.

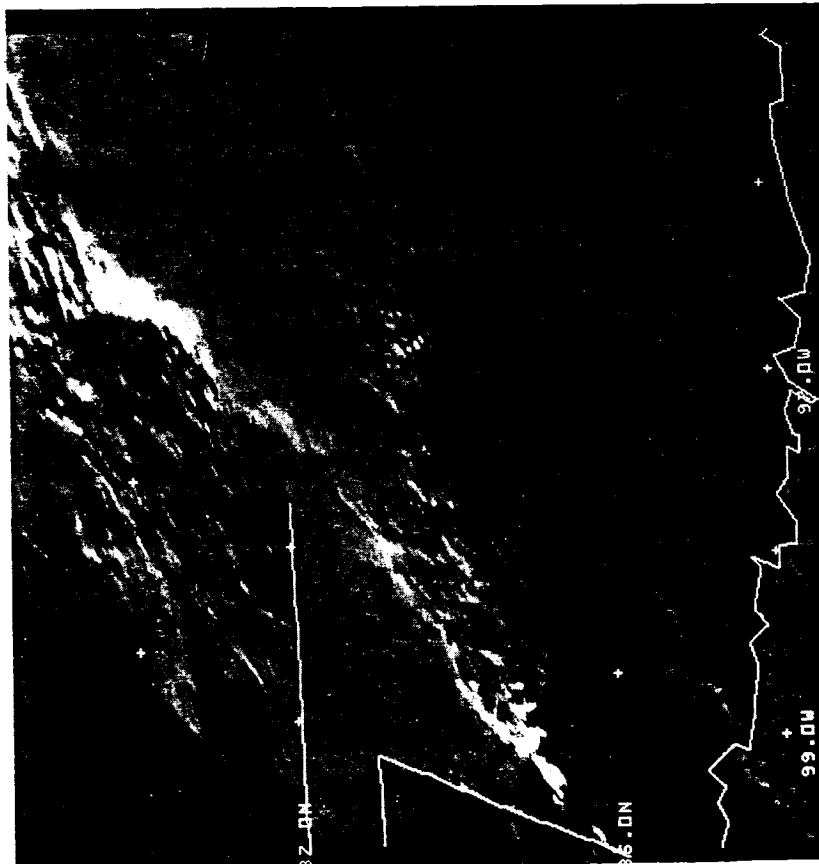


FIG. 4. GOES West image of tornadic thunderstorms in Oklahoma on 3 May 1979. The storms were scanned by the satellite at 0051:19 GMT. This image has been digitally remapped into the image coordinate system of the GOES East image (see Fig. 5) to form a stereo pair.

50B

oriented primarily in a north-south direction with no cloud contamination were used. Each area was remapped four different times and the results were averaged to reduce random line jitter and nutation effects. Again with the use of nearby coastlines as reference points, the stereo heights had a mean of 0.06 km lower than the map altitudes with a standard deviation of 0.14 km. The difference of the altitude of the coastlines from sea level (absolute height error) ranged from  $-0.67$  km to  $+0.26$  km, with an average bias error of 0.09 km (Table 1) for various points on the California, Baja, and Peruvian coasts. These data indicate that relative heights have accuracies approaching a few hundred meters for large ideal features measured to subpixel accuracy. Absolute heights accurate to about 0.5 km are possible with very high quality navigation solutions. For the cases studied to date the height resolution corresponding to one pixel of horizontal parallax has ranged from 0.7 to 0.2 km.

Stereo measurements of height ranging to over 18 km for clouds, which can move with speeds of over  $50 \text{ m s}^{-1}$  and may be diffuse, require additional verification. The easiest technique to employ for verification uses the companion infrared images to the stereo pair. Minzner *et al.* (1978) and Hasler *et al.* (1979a) have found agreement between infrared and stereo height techniques of about 1.0 km. However, because of the lack of precise knowledge about the cloud emissivity and the atmospheric temperature profile, this type of verification can only be regarded as approximate. Minzner *et al.* (1978) and Hasler and Adler (1980) have found agreement between radar and stereo heights, also to about 1.0 km. Again, this can only be regarded as a rough comparison because of inadequate resolution for radars far from the clouds, as well as side-lobe problems for radars that are close to the cloud; also the radar and satellite sensors respond differently to clouds.

Some types of verification that have the potential accuracy of the stereo heights of 0.1–0.5 km include 1) *in situ* aircraft observations, 2) ground-based or aerial photogrammetry, and 3) aircraft-borne lidar. With the use of all of these techniques observations have been made coincident with the scan-synchronized stereo observations from the severe thunderstorm days during SESAME '79 and for Hurricane Frederic on 12 September 1979. Data processing is now under way that will permit detailed comparisons of cloud height determinations.

Preliminary comparisons between lidar observations from the NASA WB-57-F aircraft and the cloud top altitude measurements of Hurricane Frederic from the stereo images show differences on the order of 0.5 km.

#### 4. Stereo observations applied to some meteorological problems

##### a. Three-dimensional cloud geometry

Minzner *et al.* (1978) used their stereo techniques to make spot measurements of cloud height and performed a 5 km vertical resolution height contour analysis for an extensive frontal cloud regime on 17 February 1975. A large fraction of cloud areas was observed to have heights in excess of 10 km in this study.

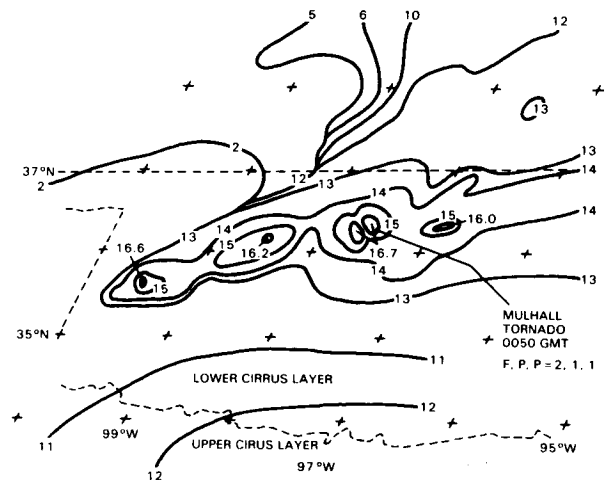


FIG. 6. Stereo cloud top height contour analysis (kilometers above sea level) made from a stereo image pair (see Figs. 4 and 5) of an Oklahoma tornadic thunderstorm complex at 0051 GMT 3 May 1979. The analysis was made using an interactive image alternation and shift technique on the Atmospheric and Oceanographic Information Processing System (AOIPS) at NASA/GSFC. See descriptive information with Figs. 4–5, the cover, and in the text. In reference to Table 3, towers 1, 0, and 1 are the highest points from left to right with altitudes of 16.6, 16.2, and 16.7 km, respectively.

Stereo techniques have been applied using the AOIPS interactive system on remapped digital images to measure cloud top heights for tornadic thunderstorms and nearby low-level cumulus and high-level cirrus in Oklahoma on 2 and 3 May 1979. Stereo heights also have been determined for the deep convective clouds near the eye of Hurricane Frederic on 12 September 1979, as well as the low-level cumulus and high-level cirrus associated with the inflow and outflow regions of the storm. Figures 4 and 5 make a stereo pair of GOES images for the severe thunderstorms in northern Oklahoma at the time a tornado was observed on the ground at 0046 GMT on 3 May 1979. Figure 5 is the GOES East image, while Fig. 4 is the GOES West image remapped into the coordinate system of the GOES East image. At this time of the day the sun casts shadows that give the overshooting towers, cirrus plumes, and other cloud top features high contrast and makes them easy to see. This image pair can be viewed stereoscopically using a stereo viewer. The same image pair is presented on the cover, where the GOES East image (red) and the remapped GOES West image (blue-green) have been superimposed for stereo viewing. In order to view this properly remove the pair of red and green stereo glasses from the insert (p. 193) and wear them with the red filter over the right eye. Hold the figure and glasses such that reflections are minimized. The grid appears slightly below the height of the anvil edge, while a line of tropopause penetrating tops running from WSW to ENE should appear highest. The most massive overshooting tops on the eastern end of the line are closely associated in time and space with a tornado damage report. Cirrus plumes, downwind (northeast) of the overshooting tops, can also be seen above the relatively level main anvil top. Two levels of upper-level cirrus clouds can be seen south of the storm. To the northwest of the storm, low-level stratus clouds slope upward to the northeast as convection becomes more intense. Figure 6 shows a stereo

cloud top height contour analysis made from the stereo image pair in the cover picture using the interactive image alternation and shift technique on AOIPS. Note that the tallest tropopause-penetrating tops at 16.7 km are coincident with the Mulhall (F2) tornado. Large anvil areas have heights above 14.0 km, while the anvil edge ranges from 12 to 13 km. The cirrus plumes downwind (northeast) of the tallest towers, with altitudes up to 16.0 km, are apparently remnants of earlier towers. These plumes, which are at various heights above the main cirrus anvil, have higher infrared temperatures than the adjacent anvil and overshooting top areas. The stereo heights are of great importance in understanding and interpreting the infrared observations of thunderstorm tops, as will be suggested in Section 4.

Figure 7 shows a short interval (3 min) time sequence of

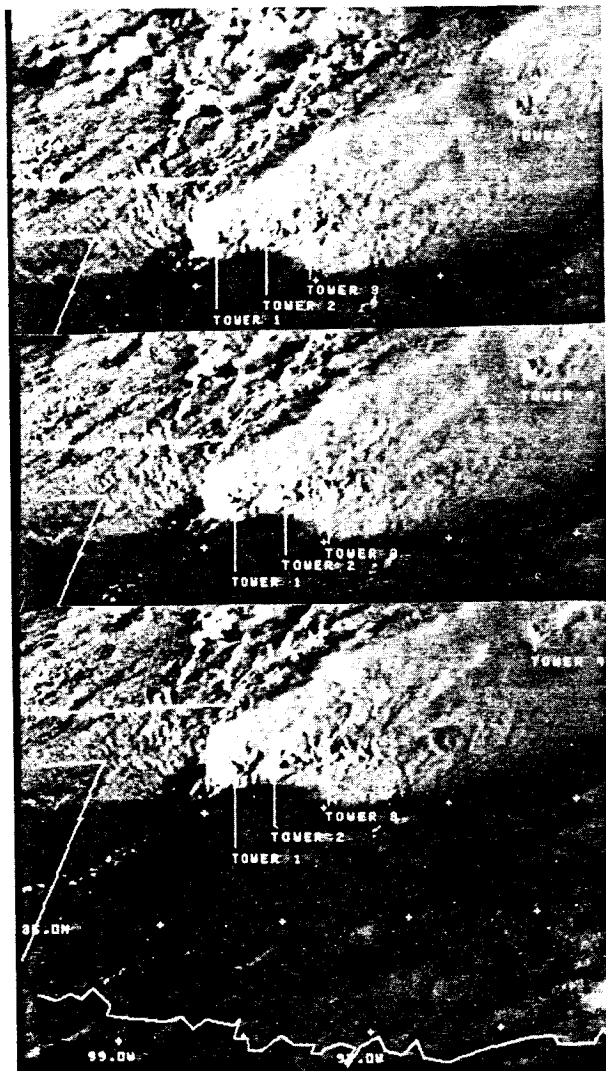


FIG. 7. Short-interval (3 min) time sequence of three GOES East images of the Oklahoma tornadic thunderstorm complex taken at 2248 (top), 2251 (middle), and 2254 GMT (bottom) on 2 May 1979, a few hours before the times of Fig. 4 and the cover picture. Note the changes in towers 1, 2, and 3 with time. A tornado was observed on the ground within a few km of tower 3 during this time period, while tower 2 had a tornado associated with it up to 2250 GMT. See Fig. 8 for stereo cloud top height contour analyses from these images together with the corresponding remapped GOES West images.

three GOES East images taken a few hours earlier at 2248, 2251, and 2254 GMT on 2 May 1979, while Figure 8 presents the stereo cloud top height contour analyses resulting from those images together with the remapped GOES West images. At 2248 and 2251 GMT two tornadoes were observed on the ground within a few kilometers of towers 2 and 3 (15.3 and 16.2 km at 2251 GMT) and mesocyclones were observed at the same locations by Doppler radar at the same time. By 2253 GMT the tornado associated with tower 2 had dissipated. Comparisons between the tallest overshooting towers, measured stereographically with radar reflectivities, Doppler radar velocities, radiosonde temperature profiles, and severe weather reports, are discussed by Hasler and Adler (1980) and in Section 4 of this paper.

Figure 9 shows a GOES East image when the sensor scanned Hurricane Frederic at 1957 GMT on 12 September

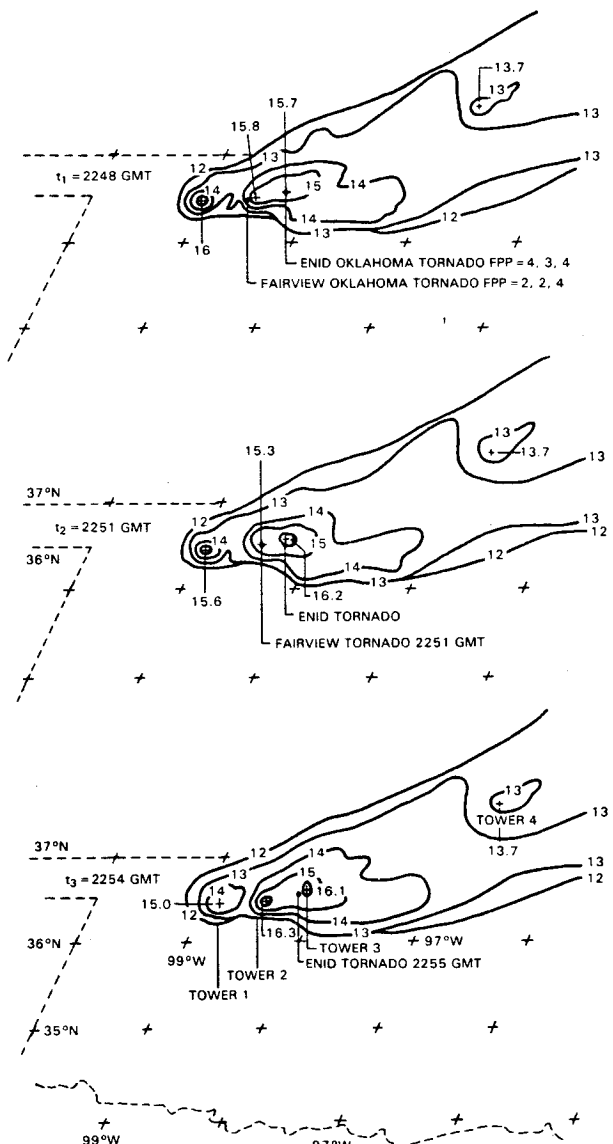


FIG. 8. Stereo cloud top height contour analyses of the images in Fig. 7 together with the corresponding remapped GOES West images. Observe the cloud top height ascent of 15.3 km to 16.3 km for tower 2 between 2251 and 2254 GMT and the descent of tower 1 from 15.6 to 15.0 km over the same 3 min period.

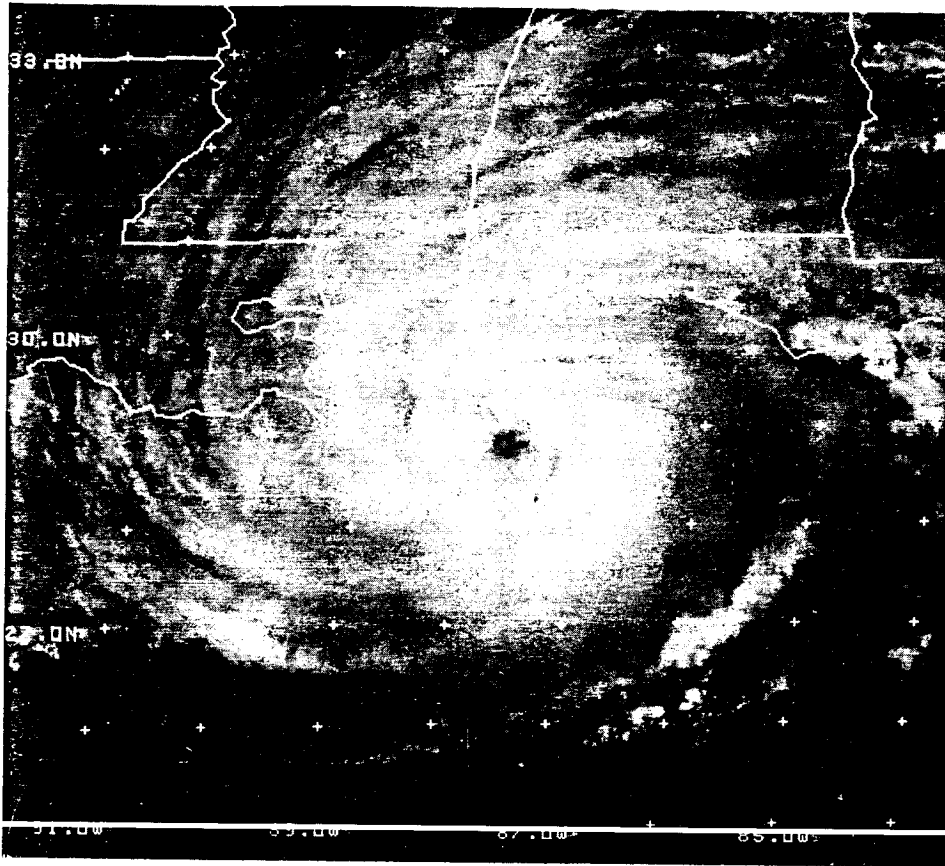


FIG. 9. GOES East image with Hurricane Frederic scanned by the sensor at 1957 GMT on 12 September 1979 as it approached the Gulf Coast near Mobile, Ala. See Fig. 10 for stereo cloud top height contour analysis based in part on this image. Features are described in the text.

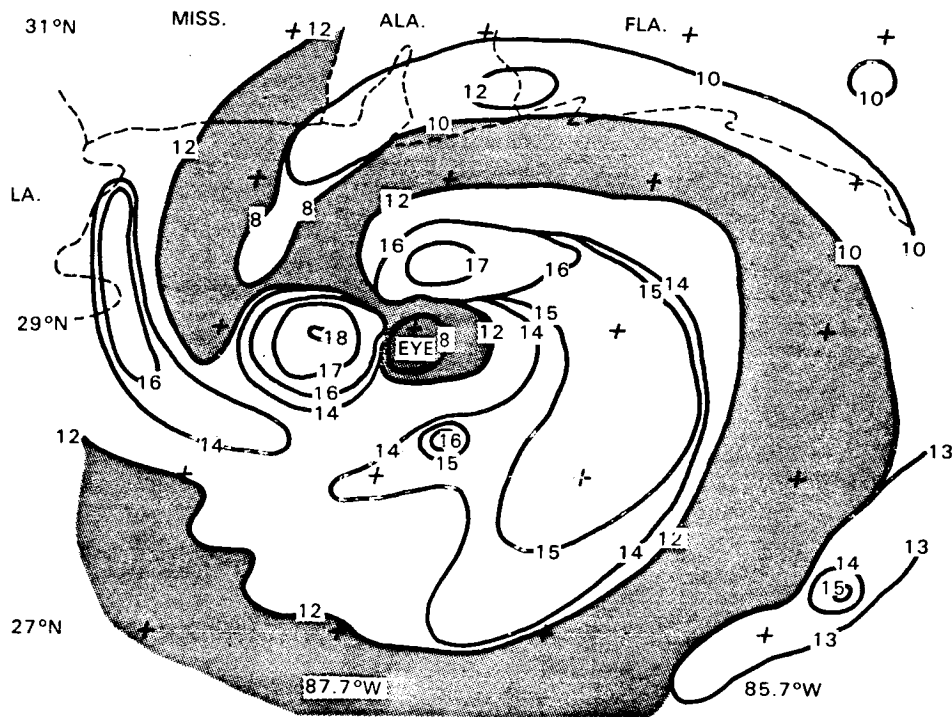


FIG. 10. Stereo cloud top height contour analysis of Hurricane Frederic at 1957 GMT on 12 September 1979, based on the simultaneous GOES East (see Fig. 9) and remapped GOES West images. An interactive image alternation and shift technique is used to analyze for constant parallax on AOIPS. See text for description of features.

1979 as it approached the Gulf Coast near Mobile, Ala. The cloud top height contour analysis from the stereo image pair at that time is given in Fig. 10. Two large convective cell areas with altitudes of 17–18 km are west and north of the eye. The cloud-free and low cloud eye observed using the stereo is about half the size of the eye as seen by radar. A large thick cirrus outflow area with altitudes of 12–15 km spirals out from the northern cell. There is a gap between the two major cells northwest of the eye, with clouds in that region observed as low as 8 km. The spiral area shaded in Fig. 10 probably contains some thin featureless high-level cirrus, but has no clouds whose height could be measured using stereo. At larger radii, the spiral bands have elevations ranging from 10 km north and east of the storm to 16 km west of the storm. Analysis of short interval (7.5 min) stereo image sequences allows improvements in hurricane parameter estimation over previously used techniques. For example, 1) observations of the changes in the structure of the central dense overcast (CDO) as a function of time, 2) observation of the circulation of the storm at multiple levels from stereo cloud motion tracking and stereo wind altitude assignment, and 3) estimation of storm intensity from stereo height observations of the CDO combined with infrared cloud top temperature measurements.

#### b. Cloud top and base measurements

Figures 11 and 12 show the 2 May 1979 Oklahoma tornadic thunderstorm at an earlier stage of development (2114 GMT), when a variety of low-level cumulus and cirrus cloud heights were measured for the purpose of cloud-wind height assignment. The diagram in Fig. 13 illustrates how the height of cloud bases as well as tops can be measured for some clouds. Part A of Fig. 13 shows what a typical towering cumulus in Figs. 11 and 12 looks like from the two satellites. Since the western satellite views the cloud with a low eleva-

tion angle of about 30°, it will observe the edge of the cloud base as well as the cloud top (see Part B of Fig. 13). The eastern satellite, which observes the cloud from a higher elevation angle of about 40°, will also observe a point near the base if the cloud is not leaning to the southeast, which is not a problem on this day due to the prevailing vertical wind shear. In practice, it is not usually possible to identify specific features at the tops and bases of small clouds in the images of both satellites. Therefore, as a first approximation, points have been selected (see points T and B in Fig. 13) that would be at the tops and bases of an ideal cloud viewed from the given perspectives. Furthermore, cumulus clouds in a homogeneous air mass tend to have their bases at the same level. Thus, cloud bases can be measured for the smallest clouds in the regime, where there will be very little obscuration due to their tops. These bases can then be used for the nearby clouds in the same regime.

Table 2 shows some typical estimates of cloud top and base heights for a number of clouds used for wind estimation on 2 May 1979, which are illustrated in Figs. 11 and 12. The lowest clouds (stratus) to the southeast and west of the storm had no detectable altitude difference from ground-level reference points (0.5–0.7 km). For the low-level cumulus southwest of the storm, along which later storm growth occurred, cloud bases were 2.5 km and tops were up to 6 km. Cirrus cloud heights ranged from about 8 to 11 km, but distinct cloud base and top measurements were not usually possible. Figure 11 gives the cloud winds at four levels, which are color coded according to their height. For the stratus and cumulus clouds at 0.5, 1.5, and 2.5 km the cloud base altitude was used, while the cirrus cloud altitude of 10 km represents an approximate value for those clouds. In Fig. 12 the same information is presented in stereo, which may be viewed using red/green glasses. Cloud wind vectors appear at their approximate altitude for the regions or layer. The graphics are superimposed

TABLE 2. Satellite cloud winds with stereo height assignment compared with Oklahoma City rawinsonde winds in the vicinity of tornadic thunderstorms on 2 May 1979.

Cloud regime	Cloud winds (2113–2122 GMT)				Rawinsonde winds ~0000 GMT (5-3-79)			
	Direction (deg)	Speed (m s <sup>-1</sup> )	Cloud altitude (km)		Station	Direction (deg)	Speed (m s <sup>-1</sup> )	Altitudes (km above MSL)
			Bases	Tops				
Low-level Cu and stratus SE of storm	138–155	8–12	~0.5	~1.0	HEN OKC	180–210 160–200	5–12 7–14	0.3–1.4 0.4–1.3
Low-level stratus west and SW of storm	314–325	11–17	~0.7	~1.0	GAG	030–010	8–13	0.7–1.2
Low-level Cu south of storm	185–225	9–15	1.5	2.5–3.3	OKC	209	12.9	1.6
Cu line and low-level Cu SW of storm	229–248	15–19	2.5	4.0–5.9	OKC	236	17	~2.5
Cirrus south of storm	252–277	25–55	—	7.8–10.8	OKC	252–261	27–52	8.8–10.9
Cirrus SW of storm (a)	250	55	—	10.8	OKC	252	52.5	10.9
Cirrus SW of storm (b)	262	34	—	7.8	OKC	253	27	7.8

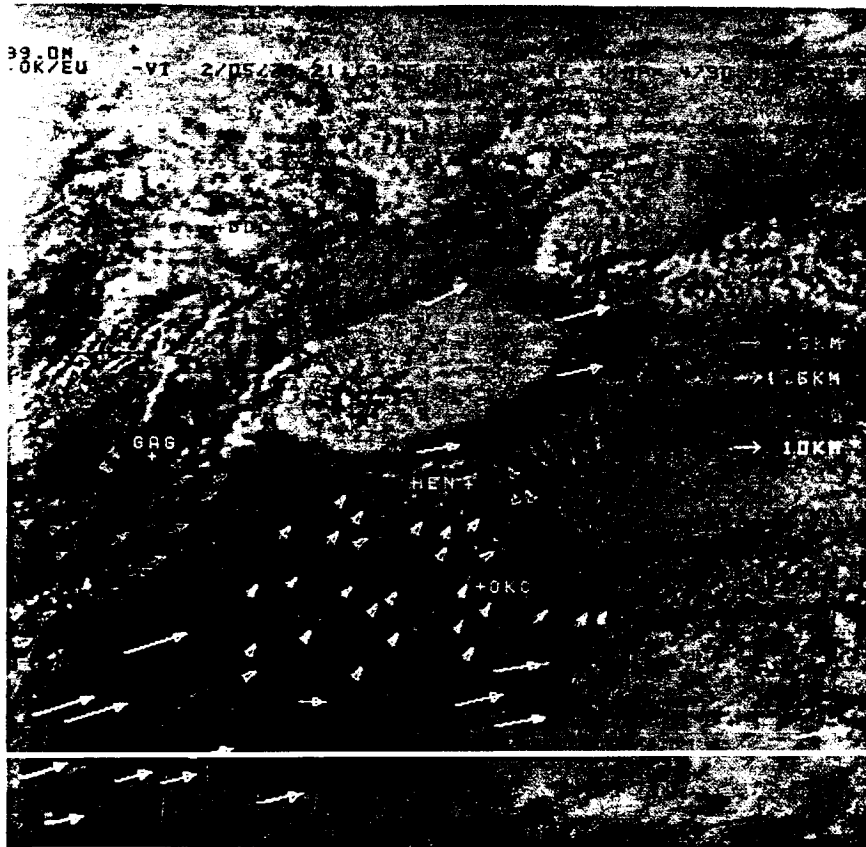


FIG. 11. Multi-level wind field estimate from GOES short-interval images using stereo height assignment for the tornadic thunderstorm complex at 2114 GMT on 2 May 1979. The legend on the right shows arrows color coded according to height with the given length representing  $10 \text{ m s}^{-1}$ .

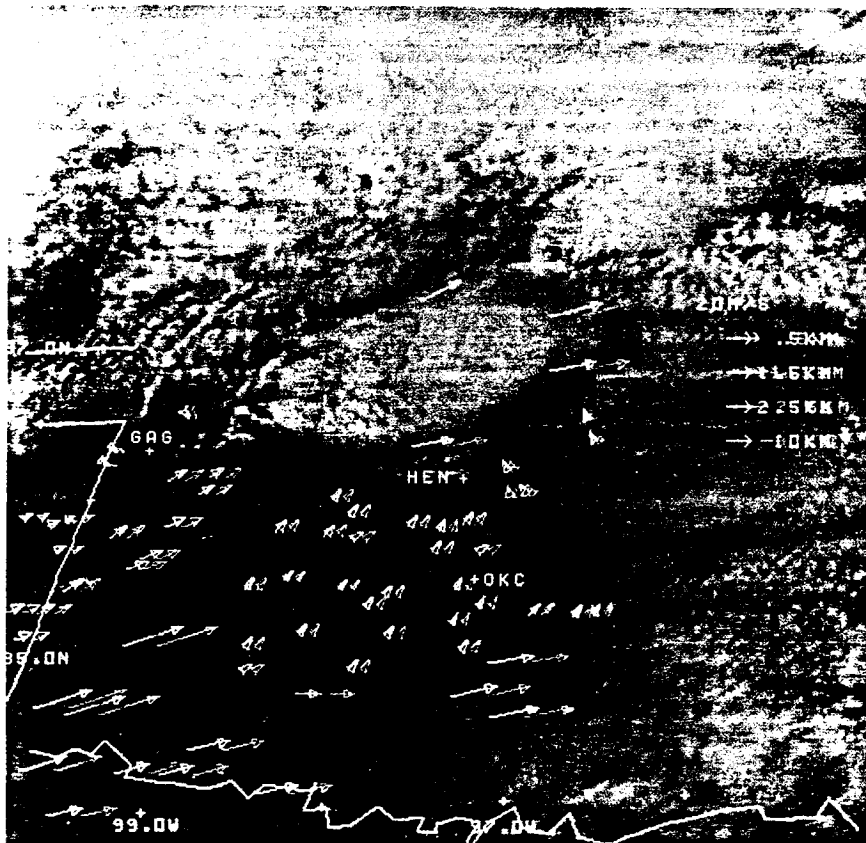


FIG. 12. Same as Fig. 11, except stereo presentation, which should be viewed with red/green anaglyph glasses. Vectors appear approximately at the height of the clouds that were tracked to estimate the winds. The stereo graphics are superimposed on an artificial stereo image constructed from the visible and infrared images using a technique similar to that of Pichel *et al.* (1973).

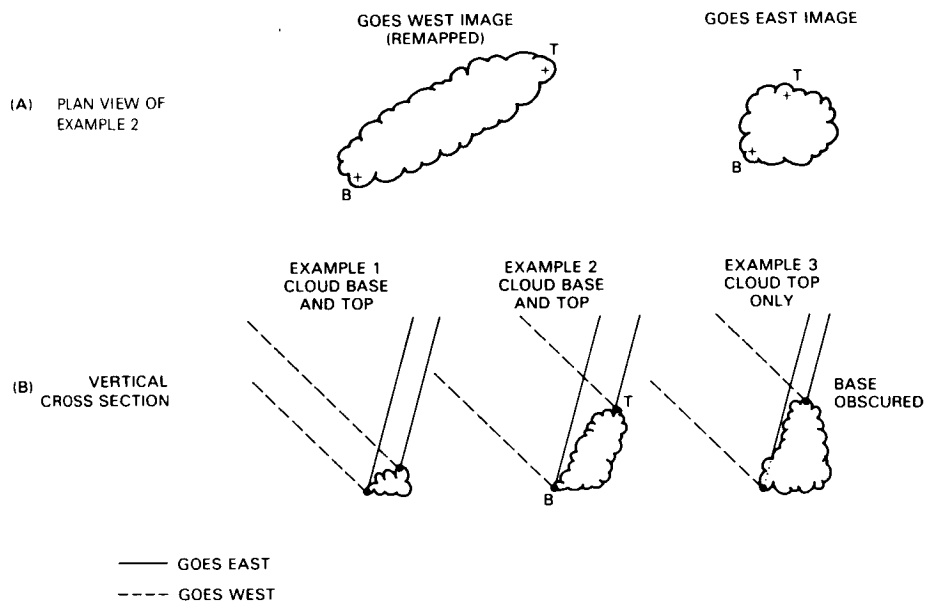


FIG. 13. Schematic illustration of cumulus top and base height measurements from stereographic observations of two geosynchronous satellites.

on an artificial stereo image constructed from the visible and infrared images using a technique similar to that of Pichel *et al.* (1973).

#### c. Cloud-wind height assignment

The cloud top and base height measurements discussed in the previous section represent a quantum jump in the ability to assign heights to winds estimated from cloud motions. Cloud base height measurements are particularly important because most cumulus cloud-winds over oceans should be assigned to the altitude of their bases (Hasler *et al.*, 1979b). Similarly, the limited comparisons between cloud motions and winds over land made by Telford and Wagner (1974) show that the best agreement is for the cloud base level or below. For cirrus and frontal cumulus clouds, Hasler *et al.* (1977) have indicated that the midcloud altitude is the proper level for wind height assignment. It is therefore apparent that both cloud top and base height measurements are important. The stereo heights are particularly important for thin cirrus clouds because of the inability of the infrared techniques to give accurate height estimates.

#### d. Dynamics of convective clouds

Time series of cloud top heights, such as the one presented in Table 3 for tropopause-penetrating cloud tops for the 2 and 3 May 1979 tornadic thunderstorms (see Figs. 7 and 8), can be used to compute cloud top ascent and descent rates. Growth rates are observed in excess of  $5 \text{ m s}^{-1}$  over 3 min for these towers well above the tropopause. These growth rates are of the same magnitude as those measured by Shenk (1974) using side-looking photography from an aircraft. The stereo cloud growth estimates have great potential for estimating the intensity of thunderstorms, with the use of techniques analogous to those employed by Adler and Fenn (1979) using in-

frared images. The higher horizontal resolution of the stereo heights and their independence from the atmospheric temperature profile are tremendous advantages for this application.

If we include the infrared cloud top temperatures from Table 3 and compare the data with the environmental temperature profile as shown in Fig. 14, additional information can be inferred about the dynamics of severe convection. In Fig. 14 the stereo cloud top height contours that have an enclosed area of at least  $100 \text{ km}^2$  are plotted against the corresponding IR temperatures of the coldest cloud tops of about the same area for the major active convective towers. Cloud temperatures derived from a 1-dimensional cloud model (Simpson and Wiggert, 1969) using the Oklahoma City, Okla. (OKC) radiosonde sounding and given a cloud diameter of 6 km are also shown. For the overshooting towers in mature thunderstorms within 100 km and 2 h of the sounding, the IR temperatures vs. stereo heights (see crosses in Fig. 14) fall between the adiabatic ( $-10^\circ\text{C km}^{-1}$ ) and the ambient ( $+3.6^\circ\text{C km}^{-1}$ ) lapse rates. The cloud temperatures given by the model indicate only a slight mixing with the environment for a cloud of this diameter, but the model gives the temperature of the relatively undiluted updraft core. On the other hand, the satellite infrared instrument does not see more than 100 m into the cloud top surface layer that is actively mixing with the environment. Further, the satellite observes over a larger area (than the rising tower), which comprises older cloudy material that has undergone substantial mixing with the surroundings. Observations from new towers on the southeast flank (circles with crosses in Fig. 14) are still closer to the environmental temperature. This is probably due to sensor field of view or time response problems that bias the observations toward higher temperatures.

Observations of this type will be valuable aids in judging how well models of different types handle the complicated

entrainment, precipitation loading, pressure effects, shear effects, etc., that govern cumulus dynamics.

*e. Atmospheric temperature from stereo heights and infrared cloud top temperatures*

In areas with favorable cloud regimes, the information from the simultaneous measurements of cloud temperature and height using infrared and stereo measurement can be used to derive atmospheric temperature with greater horizontal and vertical resolution and less ambiguity than the other satellite remote sensing techniques.

Figure 15 shows temperatures at three heights (A, C, D) derived from infrared cloud top temperatures and stereo heights; the cloud tops are presumed to be in equilibrium with the surrounding air and should have emissivities near 1.0. The stereo measurements are made from the GOES East and GOES West visible (see cover picture) and infrared images taken at approximately 0051 GMT on 3 May 1979. The 0000 GMT radiosonde soundings for 3 May at OKC and Gage, Okla. (GAG), also shown in Fig. 15, are nearly simultaneous in time and space with the satellite observations. Figure 16 shows the locations of the soundings and the points where temperatures were measured. At 2 km a temperature of 6°C was measured for stratiform clouds northwest of the storm (point A), which compares to 10°C at the same altitude and location for the GAG sounding. The thin cirrus clouds south of the storm (point B), with stereo heights of 12 km, have a temperature of -47°C, while the OKC sounding temperature is -55° at that altitude. The agreement here is poor because of the low emissivity of the cirrus clouds. The emissivity of the cirrus could be calculated from multi-channel IR data on TIROS-N or VAS (visible infrared spin-scan radiometric atmospheric sounder) which would make an estimate possible here as well. A broad shelf on the cirrus anvil south of the main turret (point C) at 12 km has a temperature of -67°C, which coincides almost exactly with the tropopause determined from the OKC sounding. Downwind (northeast) of the main turret (point D) is an area at a height of about 15 km that has a much higher infrared temperature of -60°C. This point is also in excellent agreement with the OKC radiosonde measurement of -60°C, which confirms the higher temperatures in the stratosphere. This kind of temperature profile depends on the presence of relatively high emissivity clouds. However, one would expect to have temperatures for at least two or three heights that could be used to give reference points and to give additional vertical temperature resolution to the satellite soundings that rely on inversion of the radiative transfer equations.

*f. Cloud emissivity estimation*

The addition of direct stereo cloud height observations to presently available conventional and satellite data makes it possible to obtain the accurate estimates of cloud emissivity that are needed for atmospheric radiation and climate modeling. Given observations of 1) upwelling infrared radiation at the top of the cloud,  $T_{IR}$ ; 2) upwelling radiation at the base of the cloud,  $T_c$ ; and 3) the cloud temperature,  $T_c$ ; it is possible to estimate the emissivity of the cloud.  $T_{IR}$  is obtained from the GOES infrared sensor measurements over the

cloud,  $T_c$  is approximated by taking an infrared measurement of a nearby clear area, and  $T_c$  is obtained from the closest radiosonde sounding at the cloud height given from the stereography.

The stereo heights of the thin cirrus clouds to the south of the tornadic thunderstorms in northern Oklahoma on 2 and 3 May 1979 (see cover picture and Fig. 6) were used together with the Oklahoma City sounding (Fig. 14) to give the cloud temperatures ( $T_c$ ). Upwelling radiation measurements were taken from the GOES East infrared image taken at the same time for cirrus of various thicknesses ( $T_{IR}$ ) and for the clear areas ( $T_c$ ) between the storm and the cirrus clouds. Computations of emissivity  $\epsilon$  were made using the following expression

$$\epsilon = \frac{\int_{\lambda_1}^{\lambda_2} \psi_{\lambda} B_{\lambda}(T_{IR}) d\lambda - \int_{\lambda_1}^{\lambda_2} \psi_{\lambda} B_{\lambda}(T_c) d\lambda}{\int_{\lambda_1}^{\lambda_2} \psi_{\lambda} B_{\lambda}(T_c) d\lambda - \int_{\lambda_1}^{\lambda_2} \psi_{\lambda} B_{\lambda}(T_s) d\lambda}$$

where  $B_{\lambda}(T)$  is the Planck function, which is integrated over the spectral range of the GOES infrared detector from wavelength  $\lambda_1 = 10.5 \mu\text{m}$  to  $\lambda_2 = 12.5 \mu\text{m}$ ; and  $\psi_{\lambda}$  is the detector efficiency, which is assumed to be a constant.

Emissivity estimates ranged from  $\epsilon = 0.9$  for the thicker clouds to  $\epsilon = 0.2$  for the thin ones. For the low emissivity clouds, large errors in cloud wind height assignment could be made with use of present infrared height techniques, since the stereo observations of cloud height show variations of over 3 km.

*g. Stereo observations of overshooting thunderstorm towers vs. radar and surface observations of severe weather*

Between 2114 GMT on 2 May and 0053 GMT on 3 May 1979, a large number of stereo cloud height measurements were made for a severe thunderstorm complex in northern Oklahoma. Ground survey teams verified that five tornadoes were produced by this system during this period (Alberty *et al.*, 1979). The tallest and most massive overshooting towers, with stereo heights of 15-17 km, were observed to be within a few kilometers of all five tornadoes observed at the same time on the ground (see Figs. 6 and 8 and Table 3).

For example, in Fig. 8 towers 2 (15.8 km) and 3 (15.7 km) were directly above the Fairview (F2) and Enid (F4) tornadoes, respectively, at the time of the satellite scan (2248 GMT). About two hours later, at 0050 GMT on 3 May, the most massive overshooting tower, with a maximum height of 16.6 km, was directly above the Mulhall (F2) tornado observed at the same time, as shown in Fig. 6.

Digitized National Severe Storms Laboratory (NSSL) WSR-57 and Doppler radar reflectivity scans from Norman, Okla., for 0°, 3°, 4°, 5°, 5.5°, and 6° elevation angles have been remapped to the GOES satellite images. The 4° and 5.5° elevation Doppler radar scans are shown superimposed on the GOES image scanned at 2248:22 GMT ( $t_1$ ) in Figs. 17 and 18 respectively. The 4° scan at 2248:28 GMT barely intercepts the top of a precipitation area that coincides exactly with tower 1 (see Fig. 7) as seen by the satellite 45 s earlier in the GOES image. The 5.5° elevation scan at 2245:25 GMT barely intersects the top of a precipitation area a few kilometers east of tower 2 and gives a return from a somewhat larger

TABLE 3. Maximum stereo cloud top heights and lowest infrared temperatures observed from geosynchronous satellites, and times of the tornadoes associated with them for tropopause-penetrating thunderstorms on 2 and 3 May 1979. Both the highest point and the height of the contour enclosing at least at 100 km<sup>2</sup> area are given. The number in parentheses is the number of pixels at each lowest temperature having an area of about 100 km<sup>2</sup>.

Image time (GMT)	Tower -1		Tower 0		Tower 1		Tower 2	
	Height (km)	Temp. (°C)	Height (km)	Temp. (°C)	Height (km)	Temp. (°C)	Height (km)	Temp. (°C)
2115							12.6/12.1	-51*
2118							13.0/12.1	-54*
2121							12.6/12.6	-57*
2124							13.0/12.1	-59*
⋮							⋮	⋮
2142						-25.5(1)		-60*
2145						-34(1)		-62*
2148						-37(1)		-64*
2151						-40(1)		-65(1)
2154						-44(1)		-67(2)
⋮								⋮
2215					13.6/12.6	-61(3)	T <sub>1</sub> 15.9/14.5	-69(2)
2218					13.6/12.7	-62(3)	15.9/14.5	-69(3)
2221					14.5/13.6	-64*	15.9/14.5	-67(7)
2224					⋮	-64*	⋮	-68(2)
⋮					⋮	⋮	⋮	⋮
2245					16.0/14.1	-64*	15.7/14.4	-68(20)
2248					15.7/14.5	-65(1)	15.8/15.3	-69(10)
2251					14.7/14.9	-63*	16.3/15.9	-71(1)
⋮					⋮	⋮	⋮	⋮
2300						-68*		-71(2)
⋮						⋮		⋮
2306						-71(4)		
2309						-71(2)		
⋮						⋮		⋮
2330		-49(1)		-45(1)		-71(8)		
⋮		⋮		⋮		⋮		⋮
2336		-52(1)		-54(3)		-71(7)		
2339		-55(1)		-59(1)		-71(8)		
2342		-57(3)		-61(5)		-71(4)		
2345		-60(2)		-62(3)		-71(4)		
2348		-60(5)		-62(5)		-71(6)		
2351		-60(7)		-62(14)		-71(2)		
⋮		⋮		⋮		⋮		⋮
0030	16.1/15.2	-62(6)	16.6/15.6	-73(8)	16.8/15.9	-73(10)		
⋮								
⋮								
0047	—	-64(8)	15.7/14.8	-73(3)	T <sub>2</sub> 16.8/15.8	-74(2)		
0050	16.6/15.6	-67(2)	16.2/15.8	-73(8)	16.7/15.9	-74(4)		
0053	16.1/15.1	-64(10)	15.7/14.7	-73(10)	16.3/15.5	-74(1)		

\*Not closed isotherm.

area coinciding almost perfectly with tower 3.

The National Center for Atmospheric Research's (NCAR) Doppler radar located at Roman Nose, Okla., was only 45 km from tower 2 at time  $t_1$ . Preliminary calculations show good agreement between the locations of towers 2 and 3 determined from the stereo and the positions of two mesocyclones observed on the 1.5° elevation scan. The mesocyclone corresponding to tower 2 had horizontal shear of  $\sim 8 \times 10^{-3} \text{ s}^{-1}$  calculated over 5 km, while the mesocyclone corresponding to tower 3 had similar shear over 9 km. The reflectivity measurements from the radar also show a definite hook echo associated with tower 2 on the 1.5° elevation scan at 2246:20 GMT. The position of tower 1 in the satellite images also agrees to within a few kilometers of the center of an apparent

weak mesocyclone. Since the mesocyclones corresponding to towers 2 and 3 also appear in the 3.5° scans there is evidence of vertical continuity.

## 5. Summary

### a. Conclusions

Observations of cloud geometry using scan-synchronized stereo geostationary satellite images with horizontal spatial resolution of about 1.0 km, vertical resolution of approximately 0.5 km, and temporal resolution of up to 3 min pro-



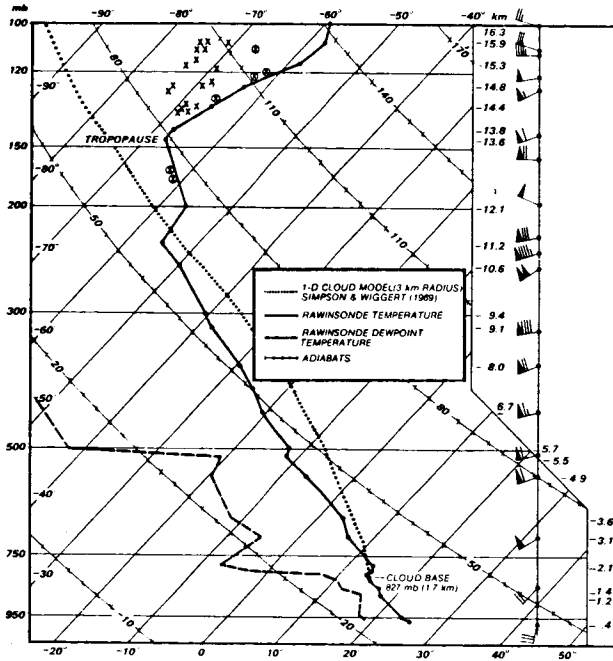


FIG. 14. Skew T-Log P diagram of the following: 1) the rawinsonde sounding at 0000 GMT on 3 May 1979 from Oklahoma City, Okla.; 2) cloud temperatures given by a 1-dimensional model using a cloud of 6 km diameter after Simpson and Wiggert (1969); and 3) highest cloud top height contours from GOES stereo measurements that enclose  $\geq 100 \text{ km}^2$  area for tropopause-penetrating severe thunderstorms plotted against the corresponding minimum infrared cloud top temperatures ( $^{\circ}\text{C}$ ) (see crosses). Satellite observations from 2214 GMT 2 May to 0053 GMT 3 May.

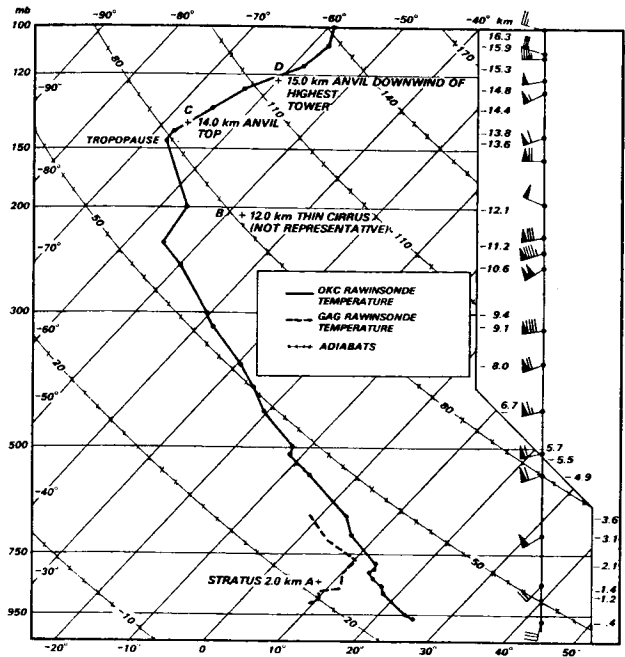


FIG. 15. Temperature ( $^{\circ}\text{C}$ ) vs. height information derived from the infrared cloud top temperature of clouds in equilibrium with the ambient air and heights derived from stereo observations at 0051 GMT on 3 May 1979. Temperatures measured for high emissivity clouds (A, C, D) agree well with nearby soundings, while temperature B, taken from thin cirrus, diverges significantly. The locations of the temperature, wind, and height measurements at 0000 GMT on 3 May 1979 at Oklahoma City, Okla. (OKC), and temperature measurements for Gage, Okla. (GAG), are also shown.



FIG. 16. Locations of rawinsonde soundings and observations of infrared cloud top temperature and stereo height for the atmospheric temperature profile derivation shown in Fig. 15.

1) The short interval (3-7 min) synchronized GOES East/GOES West imagery should be continued for exceptional severe thunderstorm days, for hurricanes in the

Gulf of Mexico, and for special experiments so that further demonstrations of the value of stereo measurements can be made.

2) A third GOES satellite should remain permanently at a longitude of about  $105^{\circ}\text{W}$ , where the recently launched GOES 4 (VAS) satellite is located. This would 1) reduce the longitude separation of two satellites from  $60^{\circ}$  to  $30^{\circ}$  and, therefore, increase the probability of observing the same feature from both satellites; 2) give better minimum horizontal resolution for both satellites over the United States; and 3) extend stereo coverage to the northeastern United States and farther east for hurricane and major east coast winter storm coverage.

3) Operational scan synchronization of all GOES satellites should be undertaken as soon as is practical, and stereo height measuring capability at key NOAA/NESS facilities such as Washington, Miami, and Kansas City should be installed as soon as practicable.

4) On a larger time scale, future geosynchronous satellites should have better resolution visible and infrared sensors so that stereo performance would be improved during the day and extended to 24 h coverage. Hasler *et al.* (1979a) have shown that stereo using infrared images is possible, but only marginally useful with the present resolution. Visible sensors with high sensitivity

for moonlight observations such as those used on the military weather satellites would also improve performance during nighttime hours.

### c. Future work

The stereo observations are being applied actively to severe storms research problems at GSFC. Major emphasis is being placed on the cloud top dynamics of severe thunderstorms and deep convection associated with hurricanes, as well as cloud wind height assignment for mesoscale wind field estimation.

Further verification of stereo cloud height accuracies is being made using *in situ* aircraft observations during SESAME. The stereo observations made during 1974, when the satellites were separated by only 30° of longitude, as well as tests envisioned with the new GOES 4 satellite near 105°W, will be evaluated to determine the advantages of more nearly identical viewing angles.

**Acknowledgments.** The author is indebted to Prof. V. E. Suomi, who conceived the Spin-Scan Camera, which has the geometric precision to do stereography from geosynchronous orbit. Suomi was contemplating making stereo measurements with a single satellite in 1965, even before his first camera was launched on a geosynchronous satellite and, as my thesis advisor, kindled my interest in working with this exciting new tool. The foresight and support of Bill Shenk, who pioneered the geosynchronous satellite stereography and synchronized the SMS satellites, is greatly appreciated. The author wishes to acknowledge the work of Mary desJardins, who developed the data-processing systems to perform the digital stereo remapping. She also wrote the software packages for interactive display and analysis of the stereo data on AOIPS and conceived the unique iterative algorithm that is used for height measurement. Without the data provided by Shenk and the software that desJardins has written, this work would not have been possible. Bob Adler shared his expertise on the structure of severe storm cloud tops. Joanne Simpson contributed her vast experience with convective dynamics, and Gerry Heysmsfield helped with the interpretation of the radar data. Ed Rodgers collaborated on the analysis of Hurricane Frederic. Gerard Szejwach made the calculations for estimation of cloud emissivity. Ray Minzner was instrumental in the early work that demonstrated the feasibility of the geosynchronous satellite stereography. Lilly Chen of General Software Corporation performed the critical navigation of the two satellites, and John Taylor and Ray Morris of GE Matsco performed the extensive data-processing tasks that were essential to this work. Andy Negri, Bill Shenk, Joanne Simpson, and Mary desJardins reviewed the manuscript and made many helpful suggestions, which have been incorporated. Finally, Sharon Felesky's fast and accurate typing and the help of Lee Dubach made the burden of producing the final manuscript much lighter.

### References

- Adler, R. F., and D. D. Fenn, 1979: Thunderstorm intensity as determined from satellite data. *J. Appl. Meteorol.*, **18**, 502-517.
- Alberty, R. L., D. W. Burgess, C. E. Hane, and J. F. Weaver, 1979: SESAME 1979 operations summary, project Severe Environmental Storms and Mesoscale Experiment. NOAA/ERL, Boulder, Colo., 203 pp.
- Black, P. G., 1977: Some aspects of tropical storm structure revealed by hand held camera photographs from space. *Skylab Explores the Earth*, NASA, Washington, D.C., pp. 417-461.
- Bristor, C. L., and W. Pichel, 1974: 3-D cloud viewing using overlapped pictures from two geostationary satellites. *Bull. A. Meteorol. Soc.*, **55**, 1353-1355.
- Bryson, W., 1978: Cloud height determination from geosynchronous satellite images. Ph. D. thesis, University of Wisconsin, 91 pp.
- Chen, L., 1980: METPAK/navigation system user's guide and study report. Prepared for Goddard Space Flight Center, Greenbelt, Md., under contract NAS5-25548. General Software Corporation, 15216 Watgater Rd., Silver Spring, Md. 20904.

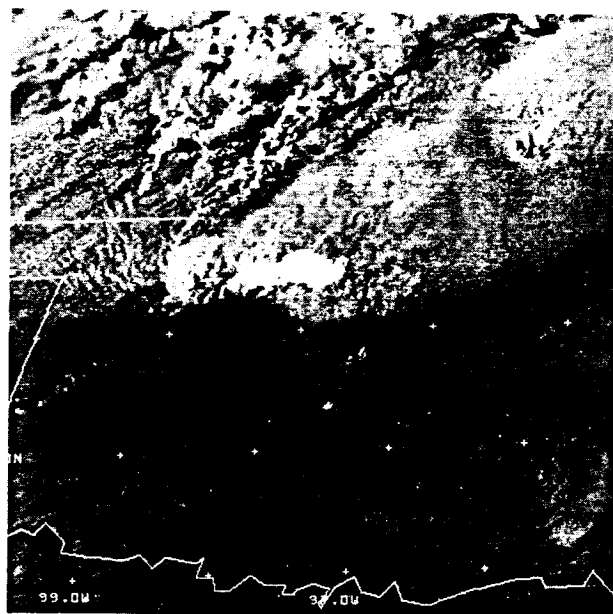


FIG. 17. Tornadic storm scanned at 2248:22 GMT on 2 May 1979 by GOES East (also shown at top of Fig. 7). Digitally remapped reflectivities from the 4° elevation scan of the NSSL Doppler radar are superimposed for a cloud height of 15 km.

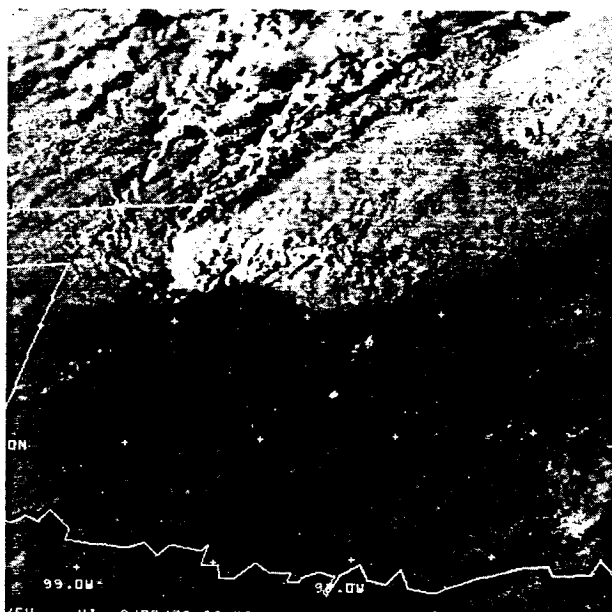


FIG. 18. Same as Fig. 17, except 5.5° elevation scan at 2245:25 GMT.

- Dalton, J. T., M. L. desJardins, A. F. Hasler, and R. A. Minzner, 1979: Digital cloud stereography from geostationary orbit. *Proceedings of the 13th International Symposium on Remote Sensing of Environment*, Environmental Research Institutes of Michigan, Ann Arbor, Mich., 23-27 April 1979, pp. 1479-1488.
- desJardins, M., 1978: Three-dimensional observations of cloud motion using interactive stereo displays. NASA/GSFC PIP presentation, 10 July 1978. (Unpublished manuscript.)
- Hasler, A. F., and R. F. Adler, 1980: Cloud top structure of a tornadic thunderstorm from 3 min interval stereo satellite images compared with radar and other observations. *Preprints, 19th Conference on Radar Meteorology (Miami Beach)*, AMS, Boston, pp. 405-412.
- , W. E. Shenk, and W. C. Skillman, 1977: Wind estimates from cloud motions: Preliminary results of Phases I, II, and III of an *in situ* aircraft experiment. *J. Appl. Meteorol.*, **15**, 812-815.
- , M. desJardins, and W. E. Shenk, 1979a: Four dimensional observations of clouds from geosynchronous orbit using stereo display and measurement techniques on an interactive information processing system. *Fourth National Aeronautics and Space Administration Weather and Climate Review*, NASA/GSFC, Greenbelt, Md., pp. 67-72.
- , W. C. Skillman, W. E. Shenk, and J. Steranka, 1979b: *In situ* aircraft verification of the quality of satellite cloud winds over oceanic regions. *J. Appl. Meteorol.*, **18**, 1481-1489.
- Kassander, A. R., Jr., and L. L. Sims, 1957: Cloud photogrammetry with ground-located K-17 aerial cameras. *J. Meteorol.*, **14**, 43-49.
- Kikuchi, K., and T. Kasai, 1968: Stereoscopic analysis of photographs taken by NIMBUS II APT System. *J. Meteorol. Soc. Japan*, **46**, 60-67.
- Lorenz, D., and E. Schmidt, 1979: Verfahren zur Stereoskopischen Wolkenanalyse aus dem Weltraum. *Bildmessung u. Luftbildwesen*, **47**, 1-14.
- Malkus, J. S., and H. Riehl, 1964: *Cloud Structure and Distributions over the Tropical Pacific Ocean*. University of California Press, Berkeley, 229 pp.
- Meyer, H., 1954: Wolken photogrammetrie mit einfachen Hilfsmitteln. *Bildmessung u. Luftbildwesen*, **22**, 9-15.
- Minzner, R. A., W. E. Shenk, J. Steranka, and R. D. Teagle, 1976: Cloud heights determined stereographically from imagery recorded simultaneously by two synchronous meteorological satellites, SMS-1 and SMS-2. *EOS*, **57**, 593.
- , —, —, and —, 1978: Stereographic cloud heights from imagery of SMS/GOES satellites. *Geophys. Res. Lett.*, **5**, 21-24.
- , —, —, and —, 1979: Stereographic cloud height from the imagery of two scan-synchronized geostationary satellites. *Fourth NASA Weather and Climate Review*, NASA/GSFC, Greenbelt, Md., pp. 61-66.
- Negri, A. J., D. W. Reynolds, and R. A. Maddox, 1976: Measurements of cumulonimbus clouds using quantitative satellite and radar data. *Preprints, Seventh Conference on Aerospace and Aeronautical Meteorology and Symposium on Remote Sensing from Satellites* (Melbourne, Fla.), AMS, Boston, pp. 119-124.
- Ondrejka, R. J., and J. H. Conover, 1966: Note on the stereo interpretation of NIMBUS II APT photography. *Mon. Wea. Rev.*, **94**, 611-614.
- Pichel, W., C. L. Bristor, and R. Brower, 1973: Artificial stereo: A technique for combining multi-channel satellite image data. *Bull. Am. Meteorol. Soc.*, **54**, 688-691.
- Roach, W. T., 1967: On the nature of the summit areas of severe storms in Oklahoma. *Quart. J. Roy. Meteorol. Soc.*, **93**, 318-327.
- Schereschewsky, P., 1921: L' Evolution de la Meteorologie. *La Nature*, 171-175.
- Shenk, W. E., 1974: Cloud top variability of strong convection cells. *J. Appl. Meteorol.*, **13**, 917-922.
- , and R. J. Holub, 1971: An example of detailed cloud contouring from Apollo-6 photography. *Bull. Am. Meteorol. Soc.*, **52**, 238.
- , —, and R. A. Neff, 1975: Stereographic cloud analysis from Apollo 6, photographs over a cold front. *Bull. Am. Meteorol. Soc.*, **56**, 4-15.
- Simpson, J., and V. Wiggert, 1969: Models of precipitating cumulus towers. *Mon. Wea. Rev.*, **97**, 471-489.
- Telford, J. W., and P. B. Wagner, 1974: The measurement of horizontal air motion near clouds from aircraft. *J. Atmos. Sci.*, **31**, 2066-2080.
- Warner, C., J. Simpson, D. W. Martin, D. Suchman, and F. R. Mosher, 1979: Shallow convection on day 261 of GATE. Mesoscale arcs. *Mon. Wea. Rev.*, **107**, 1617-1635.
- , —, G. Van Helvoirt, D. W. Martin, D. Suchman, and G. L. Austin, 1980: Deep convection on day 261 of GATE. *Mon. Wea. Rev.*, **108**, 169-194.
- Whitehead, V. S., I. D. Browne, and J. G. Garcia, 1969: Cloud height contouring from Apollo-6 photography. *Bull. Am. Meteorol. Soc.*, **50**, 522-528. ●

THUNDERSTORM CLOUD TOP ASCENT RATES  
DETERMINED FROM STEREOSCOPIC SATELLITE OBSERVATIONS

Robert A. Mack<sup>2,1</sup>  
A. F. Hasler<sup>1</sup>  
Robert F. Adler<sup>1</sup>

<sup>1</sup>Goddard Laboratory for Atmospheric Sciences  
NASA/Goddard Space Flight Center  
Greenbelt, Maryland 20771

<sup>2</sup>GE/MATSCO  
Beltsville, Maryland 20705

1. INTRODUCTION

Short interval (3 min) data from two scan synchronized geosynchronous satellites (GOES-east and GOES-west) were used to stereoscopically measure cloud top ascent rates for intense convective cells on May 2, 1979, and May 9, 1979. For comparison, vertical growth rates were also determined from simultaneous GOES infrared observations by noting the rate of change of minimum cloud top temperatures in the convective cells (Adler and Fenn, 1979). The stereoscopic technique (Hasler, 1981) provides accurate measurements of cloud top ascent rates because of the 1 km spatial resolution of the visible sensor, the independence of the stereoscopic heights from the atmospheric temperature profile and their dependence only on direct geometric measurements. Finally, a one-dimensional cloud model (Simpson and Wiggert, 1969) was used with soundings from the SESAME network on May 2, 1979, and May 9, 1979, to obtain an estimate of updraft magnitude in the storms for comparisons with the stereoscopically determined cloud top ascent rates.

2. RESULTS

2.1 Stereoscopic Observations

Fig. 1 shows two visible and infrared image pairs from GOES-east, on May 2, 1979, at 2318 GMT and 2334 GMT, of two rapidly growing towers in an intense squall line that developed south-west of two very large cells and ahead of a synoptic-scale cold front in east Oklahoma. The stereoscopically determined cloud top heights for towers 1 and 2 are plotted versus time on Fig. 2 and 3 respectively. At 2318 GMT, tower 1 was observed at 9.1 km and then rapidly rose until it neared the tropopause. At 13.2 km (0.4 km below the tropopause) the tower slowed considerably and was observed at 14.1 km, 21 min later. The ascent rate averaged over the first 9 min of the developing stage was  $7.6 \text{ m s}^{-1}$ . Tower 2 rose to 12.9 km with an ascent rate of  $10.6 \text{ m s}^{-1}$ ,

slowed to  $2.1 \text{ m s}^{-1}$  near the tropopause, reached a maximum height of 14.3 km and then collapsed. An average ascent rate over the first 9 min was  $7.7 \text{ m s}^{-1}$ .

Fig. 4 shows stereoscopic cloud top heights for a moderately growing cell on May 2, 1979, that formed to the rear of an already well developed storm in Oklahoma, 2 hours before the intense squall line developed. Stereoscopic heights indicate that the tower rose from 10.9 km to 13.3 km at a rate of  $4.4 \text{ m s}^{-1}$ . Evidence of a decrease in the ascent rate near the tropopause is indicated in the data, but more data points are needed to confirm this deceleration.

On May 9, 1979, at 2100 GMT, storm activity began ahead of a cold front in north-west Oklahoma. A sequence of four-3 min interval stereoscopic satellite images, beginning with 2117 GMT revealed two developing towers. These towers were first observed at 11.2 km and 12.0 km, 2-3 km higher than the towers on May 2, 1979. The Canadian, Texas 2005 GMT sounding indicated that the tropopause was located at about 13.0 km. Most of the ascent was observed as penetration above the tropopause. The first tower, observed at 12.0 km, penetrated the tropopause by 1.5 km with an ascent rate of  $6.9 \text{ m s}^{-1}$  and then collapsed. The second tower, first measured at 11.0 km, rose 1.1 km above the tropopause at a rate of  $5.4 \text{ m s}^{-1}$ .

Jones and Marwitz (1966) found, for developing Colorado cumulonimbus clouds, mean vertical growth rates (over  $\sim 10$  min) ranging from  $-2.23 \text{ m s}^{-1}$  to  $6.96 \text{ m s}^{-1}$  for visual top observations and  $2.54 \text{ m s}^{-1}$  to  $6.55 \text{ m s}^{-1}$  for radar echo top observations. A vertical growth rate of  $8.8 \text{ m s}^{-1}$  was calculated from maximum radar echo tops observed by Burgess and Lemon (1976) for a developing cell in the Union City, Oklahoma tornadic storm. Therefore, the magnitude of the stereoscopic derived ascent rates compares well with these past observations of intense convective cells.

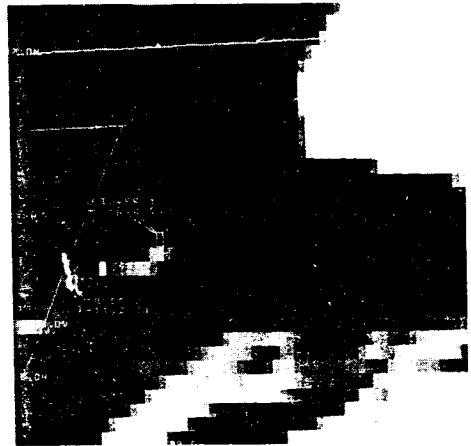
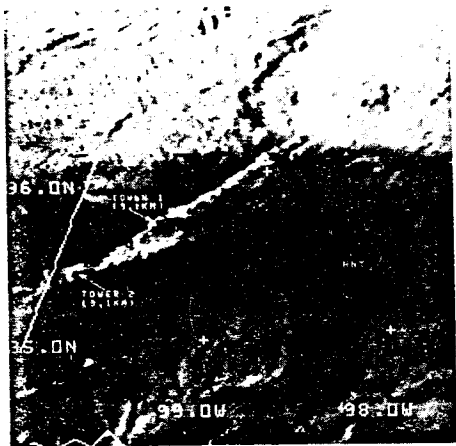


Figure 1. GOES-east visible and infrared image pairs of the developing squall line at 2318 GMT (above) and 2334 GMT (below) on May 2, 1979. The location of the rawinsonde station at Hinton, Oklahoma is shown in the 2318 GMT visible image.

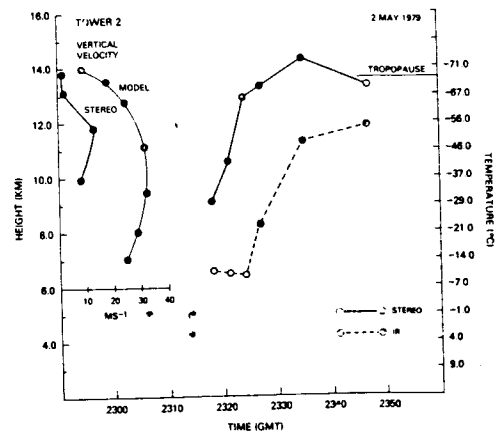
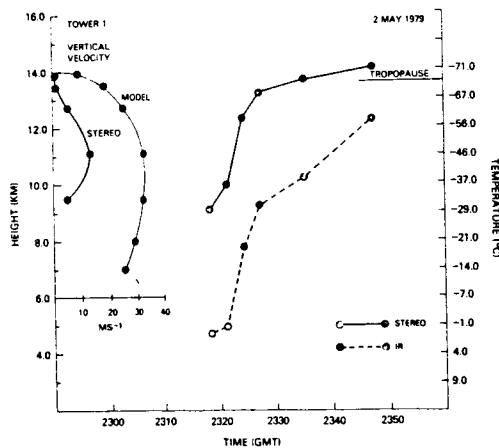


Figure 2. Stereoscopically determined cloud top heights and minimum cloud top temperatures ( $T_{BR}$ ) determined from GOES IR data for tower 1 are plotted versus time on the right-hand side of the figure. Open circles are poorly defined  $T_{BR}$ 's. Stereoscopically derived ascent rates and one-dimensional cloud model estimates of vertical velocity at different levels are shown on the left-hand side of this figure.

Figure 3. Same as Figure 2, but for tower 2.

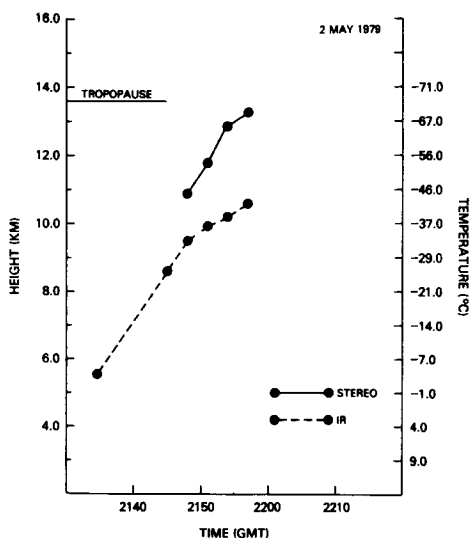


Figure 4. Stereoscopically determined cloud top heights and minimum cloud top  $T_{BB}$ 's derived from GOES IR observations for a moderate tower at 2147 GMT on May 2, 1979.

## 2.2 GOES IR Observations

Minimum cloud top equivalent black-body temperatures ( $T_{BB}$ ) were determined for each case from the GOES IR data. The  $T_{BB}$ 's were converted to heights by using the wet adiabat passing through the LCL determined by the soundings selected for each case. Figs. 2, 3 and 4 also show  $T_{BB}$  plotted versus time for the May 2, 1979 storm cases. All cases show that the cloud top heights determined from  $T_{BB}$  are much lower than the derived stereoscopic heights. They range from 13% to 39% (1.9 to 5.0 km) lower than the stereo heights for tower 1, 11% to 53% (1.4 to 6.8 km) lower for tower 2 and 13% to 22% (1.4 to 2.9 km) lower for the moderate case. This height discrepancy decreases as the towers grow higher. Heymsfield et al. (1981) found stereoscopic heights were 15% higher than the corresponding  $T_{BB}$  on May 2, 1979, for mature storms. The reason for this systematic difference is the low spatial resolution (10 km at this latitude) and possible sensor response problems of the GOES IR sensor (Adler et al., 1982; Negri et al., 1976). During the growing stage the satellite radiometer receives a contribution to the radiance from the side of the cloud and probably even the Earth's surface. Thus there is a large difference between the IR-based height and the smaller scale stereoscopic height. As the storm hits the tropopause the anvil spreads out and the effect of the satellite radiometer "seeing" the side of the cloud and/or the ground diminishes, producing less of a difference between the two height estimates. Growing storms below about 10.0 km are difficult to define in the GOES IR data as shown in Figs. 2, 3 and 4.

At 2318 GMT tower 2 (Fig. 3) was observed with a  $T_{BB}$  of  $-11.2^{\circ}\text{C}$  and barely changed ( $+1.0^{\circ}\text{C}$ ) over the next 6 min, while the stereo showed a height increase of 3.8 km. In the next 3 min the  $T_{BB}$  rapidly decreased to  $-23.2^{\circ}\text{C}$ , a rate of  $4.3^{\circ}\text{C min}^{-1}$  or a cloud top ascent rate of  $8.7\text{ m s}^{-1}$ . The graph clearly shows that the

$T_{BB}$  lags behind the stereoscopic cloud top heights. Tower 1 (Fig. 2) shows a similar behavior.

The moderate tower (Fig. 4) was first observed with stereo data at 10.9 km and the IR data showed a relatively colder temperature ( $-32^{\circ}\text{C}$ ) than was previously observed in tower 1 or tower 2 at similar heights. Possible explanations for this could be (1) the tower was larger in this case, or (2) the background in the IFOV was colder than previous cases. All explanations relate to poor IR sensor resolution.

Growth rates were determined from the  $T_{BB}$  values avoiding periods when the towers were not well defined. Tower 1 (Fig. 2) decreased in temperature at a rate of  $5.1^{\circ}\text{C min}^{-1}$  or a vertical growth rate of  $10.2\text{ m s}^{-1}$ . Tower 2 (Fig. 3) showed a temperature change of  $3.7^{\circ}\text{C min}^{-1}$ , which converts to a vertical growth rate of  $7.4\text{ m s}^{-1}$ , over the 7 min time interval starting at 2327 GMT. The moderate tower (Fig. 4) showed a  $1.1^{\circ}\text{C min}^{-1}$  temperature change or a vertical growth rate of about  $2.2\text{ m s}^{-1}$ . IR vertical growth rates of  $6.0\text{ m s}^{-1}$  and  $5.3\text{ m s}^{-1}$  were found for the first and second towers respectively on May 9, 1979, but the accuracy is questionable due to the presence of a jet stream cirrus over the towers during much of the observation period, making it difficult to get cloud top temperature measurements. IR vertical growth rates were roughly equal to stereoscopic ascent rates in the upper troposphere and greater than stereoscopic ascent rates in the storm's mature phase.

## 2.3 Model Comparison

The Simpson and Wiggert (1969) one-dimensional cloud model was run using the May 2, 1979 Hinton, Oklahoma 2325 GMT sounding (Fig. 5) and various updraft radii ranging from 1.0 to 5.0 km. The maximum observed stereoscopic height of 14.1 km corresponds to a model cloud maximum height calculated with an updraft radius of 3.0 km. Fig. 5 also shows the temperature at various levels of a rising parcel in a model cloud of 3 km radius. The vertical velocity produced by the model and the stereoscopic derived ascent rates are shown versus height on Fig. 2 for tower 1 and Fig. 3 for tower 2 on May 2, 1979. The vertical velocity estimates by the model are interpreted as the maximum vertical velocity of an air parcel in the mature thunderstorm. It is not directly comparable to the cloud top ascent rate in the growing storm. The model shows a maximum vertical velocity of  $33.2\text{ m s}^{-1}$  at 10.2 km (Fig. 5). Heymsfield et al. (1981) reported 40-50  $\text{m s}^{-1}$  updraft magnitudes in preliminary triple Doppler calculations in a similar storm in the same squall line. The stereoscopic observations show a maximum ascent rate of  $12.8\text{ m s}^{-1}$  at 11.1 km for tower 1 (Fig. 2) and  $12.7\text{ m s}^{-1}$  at 11.7 km for tower 2 (Fig. 3). The average vertical velocity from the cloud model for the layer from 9.1 km to 13.2 km was  $30.3\text{ m s}^{-1}$  or roughly 4 times larger than the stereoscopic derived ascent rates for towers 1 and 2. Woodward (1959) found in laboratory experiments that for an isolated thermal the vertical velocity in the center is about 2.2 times that of the cap. Adler et al. (1982) found by comparing an aircraft radiometer-measured ascent rate and one-dimensional cloud model results for

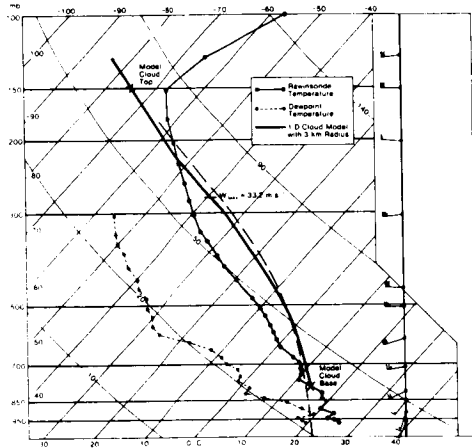


Figure 5. Thermodynamic diagram of the vertical distribution of temperature and dewpoint from Hinton, Oklahoma at 2325 GMT on May 2, 1979. The  $22^{\circ}\text{C}$  moist adiabat is shown by the long-dashed line. The thick solid line shows the vertical distribution of temperature for a rising parcel in the one-dimensional model with 3 km radius. A full wind barb is  $10\text{ m s}^{-1}$ .

a relatively weak storm that the top ascent rate was half the vertical velocity. Our results suggest that (1) this relation does not hold for intense convective storms, or (2) the model grossly overestimates the vertical velocity in this layer. The stereoscopic ascent curve suggests that the vertical velocity should gradually drop off in this layer and perhaps this is more realistic than the sharper decrease shown by the models.

The one-dimensional cloud model was run using the May 9, 1979 Canadian, Texas 2005 GMT sounding. The maximum observed stereoscopic height of 14.5 km corresponds to the model cloud maximum height having a cloud radius of 3.0 km. A maximum vertical velocity of  $31.6\text{ m s}^{-1}$  was found at 11.3 km. The average vertical velocity from the cloud model for the layer of interest was  $24.0\text{ m s}^{-1}$  or 3-4 times larger than the stereoscopically measured cloud top ascent rates.

### 3. SUMMARY AND CONCLUSIONS

The objective of this study was to measure cloud top ascent rates for growing convective cells using the satellite stereoscopic technique and to determine by comparison with growth rates determined by GOES IR temperature change and one-dimensional cloud model estimated vertical velocities, whether stereoscopic ascent rates give useful information on the intensity of these cells. Stereoscopically derived ascent rates, with approximate accuracy of  $\pm 1.3\text{ m s}^{-1}$  over 9 min, ranged from  $4.4\text{ m s}^{-1}$  for a moderate storm to  $7.7\text{ m s}^{-1}$  for a very intense storm. Stereoscopic ascent rates are comparable in magnitude to previous measurements of ground-viewed visible cloud ascent rates and radar-observed echo top ascent rates. Comparison with the rate of change of minimum cloud top temperature shows: (1) GOES IR cloud top temperatures grossly underestimate the actual cloud top height observed stereoscopically, especially for immature storms, (2) growing storms below about 10 km are difficult to define in the GOES IR data,

(3) the IR height usually lags the actual (stereo derived) one, and (4) IR determined ascent rates during the rapidly growing phases are of roughly the same magnitude of the stereoscopic derived rates.

Comparisons of stereoscopic cloud ascent rates and one-dimensional cloud model results show that the model estimated vertical velocity is 3 to 4 times greater than the top ascent rate for intense convective cells. The models maximum vertical velocity was found to be roughly at the same height as the maximum stereoscopic ascent rate.

### 4. ACKNOWLEDGEMENTS

The authors would like to thank Dr. Gerry Heymsfield and Mr. Roy Blackmer for their help in preparing the satellite data for May 2, 1979, and acknowledge the expert typing of Teresa Campbell.

### 5. REFERENCES

- Adler, R. F., and D. D. Fenn, 1979: Thunderstorm vertical velocities estimated from satellite data. *J. Atmos. Sci.*, 36, 1623-1826.
- Adler, R. F., M. J. Markus, D. D. Fenn and W. E. Shenk, 1982: Thunderstorm top structure observed by aircraft overflights with an infrared radiometer. *Preprints, 12th Conference on Severe Local Storms*, San Antonio, Texas, Amer. Meteor. Soc.
- Burgess, D. W., and L. R. Lemon, 1976: Union city storm history. Union City, Oklahoma, Tornado of May 24, 1973. NOAA Tech. Memo. ERL NSSL-80, 35-51.
- Hasler, A. F., 1981: Stereographic observations from geosynchronous satellites: An important new tool for the atmospheric sciences. *Bull. Amer. Meteor. Soc.*, 62, 194-212.
- Heymsfield, G. M., S. Schotz and R. Blackmer, 1981: Structure of thunderstorms along a squall line on May 2, 1979. *Preprints, 20th Conference on Radar Meteorology*, Boston, Massachusetts, Amer. Meteor. Soc.
- Jones, G. W. and J. D. Marwitz, 1966: Visual and associated radar tops of thunderstorms in northeastern Colorado. *Preprints, 12th Conference on Radar Meteorology*, Norman, Oklahoma, Amer. Meteor. Soc., 366-370.
- Negri, A. J., D. W. Reynolds, and R. A. Maddox, 1976: Measurements of Cumulonimbus clouds using quantitative satellite and radar data. *Preprints, 7th Conference on Aerospace and Aeronautical Meteorology*, Melbourne, Florida, Amer. Meteor. Soc., 119-124.
- Simpson, J. and C. Wiggert, 1969: Model of precipitating cumulus towers. *Mon. Wea. Rev.*, 97, 471-489.
- Woodward, B., 1959: The motion in and around isolated thermals. *Q.J.R.M.S.*, 85, 144-151.

# Artificial Stereo Presentation of Meteorological Data Fields

A. F. Hasler<sup>1</sup>,  
M. desJardins<sup>2</sup>, and A. J. Negri<sup>1</sup>  
NASA Goddard Space Flight Center  
Greenbelt, Md. 20771

## Abstract

The innate capability to perceive 3-dimensional stereo imagery has been exploited to present multidimensional meteorological data fields. Variations on an artificial stereo technique first discussed by Pichel *et al.* (1973) are used to display single and multispectral images in a vivid and easily assimilated manner. Examples of visible/infrared artificial stereo are given for Hurricane Allen (cover) and for severe thunderstorms on 10 April 1979. Three-dimensional output from a mesoscale model also is presented.

The images may be viewed through the glasses inserted in the February 1981 issue of the BULLETIN, with the red lens over the right eye. The images have been produced on the interactive Atmospheric and Oceanographic Information Processing System (AOIPS) at Goddard Space Flight Center.

Stereo presentation is an important aid in understanding meteorological phenomena for operational weather forecasting, research case studies, and model simulations.

## 1. Introduction

The display of multidimensional data sets in an easily understood manner presents a challenge to researchers in the atmospheric sciences and to those involved in operational weather forecasting. Typically, a 2-dimensional field is contoured to display the variations of scalar values. Alternatively, data can be presented as a grey scale image or with arbitrary color assignment (false color) to increase the number of discernable levels. Perspective displays such as those made by Moninger and Nelson (1980) also have been used to portray three geometric dimensions.

Even though most people have well-developed stereoscopic (3-dimensional) perception, it has not been necessary for them to use it in viewing meteorological data fields as they have been displayed up until now. A stereograph (pair of stereoscopic pictures) can be created to display three geometric dimensions directly, whereby the third dimension (perceived as height) can be any scalar quantity. This technique, called artificial stereo, is the subject of this article.

Work by Hasler (1981) and Hasler and Adler (1980) with true stereography from two Geosynchronous Operational Environmental Satellites (GOES) has demonstrated the value of 3-dimensional imagery; unfortunately, only a small fraction of present satellite data are available in stereo. A method for combining visible and infrared satellite images to make artificial stereo pairs was developed first by Pichel *et al.* (1973). This opened up a vast library of visible/infrared image pairs for both low-orbiting and geosynchronous satellites that can be viewed stereoscopically. Examples of two

such images are presented here, including the cover photo of Hurricane Allen.

## 2. Stereo display

The image processing functions necessary to produce the artificial stereo were carried out interactively on the Atmospheric and Oceanographic Information Processing System (AOIPS) at Goddard Space Flight Center (see system description by Bracken *et al.*, 1977).

The artificial stereographic pair of images consists of an original image and a second computer-generated image. In order to generate the second picture, each picture element (pixel) in the original image is shifted to the right. The shift for each pixel is computed as a linear function of the third-dimensional scalar field. In the case of the cover photograph, the radiances (or equivalent black-body temperatures) from a corresponding infrared image were used. Both the temperature and shift range are specified by the user. The lowest temperatures receive the maximum shift, the highest temperatures the minimum.

After the shifts have been computed for each pixel in a line of data, the new corresponding image line is created. When two or more pixels are shifted to the same point in the output line, the pixel at the highest level (lowest temperature, i.e., largest shift) is used. If no data are moved to a point, the data value originally at that point is retained.

In order to view the stereograph, the original image should be directed to the right eye while the computer processed image is directed to the left eye. The front cover is a standard color print, where the original image is red and the computer-generated image is superimposed in blue-green (cyan). Glasses with matching red and blue-green filters direct each image to the proper eye. Use the cardboard glasses inserted in the February 1981 issue of the BULLETIN<sup>3</sup> with the red lens on the right eye.

Both the cover image and the image in Fig. 1 were created with shifts ranging from 0 to 20 pixels. A 20-pixel leftward shift of all the points in the processed image makes the highest cloud appear at the image surface, while all lower clouds descend below the image plane. This aids the viewer in visually merging the two images and allows a grid or graphics to be written over the image without destroying the stereo effect.

<sup>3</sup>Glasses also may be purchased; as of this writing, for \$1.50 per pair including postage and handling, from 3-D VIDEO Corp., 10999 Riverside Dr., N. Hollywood, Calif. 91602. Please refer to this article in your order. Note: This source is provided as a convenience to the reader. It does not constitute an endorsement by NASA or AMS.

<sup>1</sup>Laboratory for Atmospheric Sciences (GLAS).

<sup>2</sup>Information Extraction Division.

### 3. Applications

#### a. Visible/infrared stereo

The visible/infrared artificial stereo images contain both the brightness and texture information of the visible spectrum, plus the height (temperature) information from the infrared. The image of Hurricane Allen on the cover, viewed through the stereo glasses, shows the pseudovertical structure of the cirrus clouds in the Central Dense Overcast (CDO) as they appear to descend into the hurricane eye. Many individual convective domes can be seen in the spiral bands to the east of the storm. Numerous low-level convective clouds can be seen to the south and southwest of CDO by looking deep into the

image, while at the far lower right corner, cordlike convective bands running from NNW to SSE also appear at low levels. At the bottom center of the image, thin cirrus clouds appear at mid-, rather than high, levels, apparently due to their low emissivity. In this case the infrared has substantially lower resolution (8 km) than the visible (1 km), so a 2-dimensional quadratic smoothing function was applied to the infrared image to eliminate obvious step functions in the final product.

Figure 1 shows a visible/infrared artificial stereo display of pre-tornadic thunderstorms on 10 April 1979, as viewed from TIROS-N. In this case, both the visible and infrared images have 1 km resolution at nadir. The fine structure of the numerous tropopause-penetrating convective towers is



FIG. 1. An artificial stereo image of severe thunderstorms observed by TIROS-N at 2045 GMT, 10 April 1979. To view the image properly, use the stereo glasses inserted in the February 1981 issue of the BULLETIN, with the red lens on the right eye.

readily apparent, as are wave patterns in the anvil top in central Oklahoma. Very low-level stratus clouds are visible at the top and bottom of the image. Agreement between the small-scale features on top of the anvil is much better here than in the GOES data, where there is a large (8X) factor in resolution between the visible and infrared.

*b. Stereo display of numerical model output*

Figure 2 shows a simulation from the Drexel-NCAR 3-dimensional mesoscale primitive equation model (see Kreitzberg and Perkey, 1976; 1977) displayed in stereo and remapped onto a GOES-East visible image. Figure 2 also should be viewed with the red/blue-green glasses, with the red lens over the right eye. The simulated lower atmospheric

moisture is represented in terms of specific humidity for the severe thunderstorm outbreak of 6 May 1975, which produced the Omaha, Nebr., tornado. A stereo height scale showing the three model levels of 0.375, 1.25, and 3.00 km is found in the lower left-hand corner. The specific humidity values range from less than 2 g/kg over the dry Great Plains to 14 g/kg for moist air being transported up over the Gulf states from the Gulf of Mexico. The strong moisture gradient (dry line) running north-south through eastern Oklahoma, Kansas, and Nebraska, as indicated by the model, is reasonably well aligned with the line of severe thunderstorms slightly farther east. At the highest model level shown here (3 km) the western dry air overruns the surface dry line. Note the solid 2 g/kg line looping down into the extreme south-eastern corner of Oklahoma and into eastern Texas. This

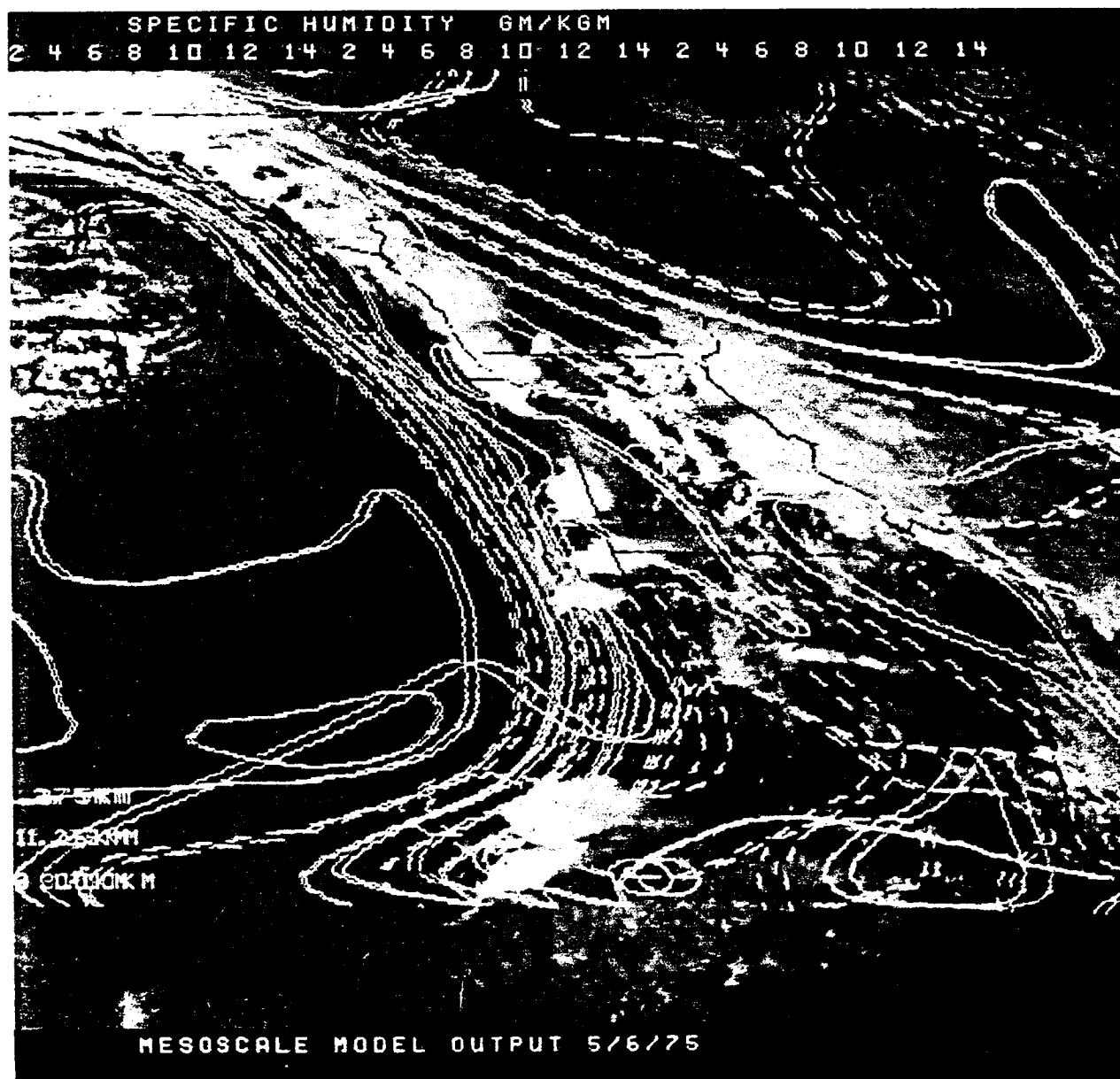


FIG. 2. Stereo image of specific humidity fields from the Drexel-NCAR 3-dimensional mesoscale model, superimposed upon satellite observations of severe thunderstorms along an intense dry line on 6 May 1975. Use stereo glasses as with Fig. 1. (Using a technique suggested by J. T.)

type of display system aids in the understanding of the 3-dimensional dynamics of the atmosphere. The combination of satellite image sequences and model simulations of convective development allows comparison and verification on small time and space scales. For a more complete description of stereographic displays of model output, the reader is referred to desJardins and Hasler (1980).

#### c. Artificial stereo/false color displays

The same algorithm used for the visible/infrared artificial stereo has been applied using the infrared as the base image as well as the coding image. In this case, it is desirable to assign false colors according to temperature in order to enhance the features. This produces color stereo pairs that require prismatic or polarizing systems for effective display. The combination of artificial stereo and false color can be used with any kind of 2-dimensional scalar field, though it works best with relatively smoothly-varying functions such as radar reflectivity and infrared images, and is applicable even if the scalar field has no direct relationship to height. By combining the artificial stereo and the false color, the hierarchy of color is obvious immediately. This allows the observer to assimilate quickly the information contained in the images.

#### 4. Summary

Principles of stereoscopic imaging and perception have been applied to develop a general method for displaying multidimensional data sets using artificial stereo. With a minimum of computer processing it is possible to obtain an artificial stereo image that has a great visual impact. The artificial stereo provides an intuitive representation of the cloud height field that can be scanned and assimilated rapidly.

Artificial stereo has one major shortcoming: It is not a true measure of cloud height, but only a measure of a scalar field, such as the equivalent black-body temperature of clouds. This means that its use is for the qualitative, not quantitative, depiction of the cloud height field. The most serious problems are caused by low-emissivity clouds (e.g., thin cirrus) and clouds that are too small to fill the instantaneous field of view of the sensor. In both cases the clouds will appear too low. However, this is generally a minor distraction that can be taken into consideration by a careful observer.

A future application of artificial stereo will involve the display of Cloud Physics Radiometer (CPR) data from a high-flying WB-57 aircraft. In this case, visible image data will be height coded using the difference between two oxygen bands. This difference is a measure of the absorption of solar radiation and therefore an indication of the depth of the intervening atmosphere.

The visible/infrared artificial stereo satellite data also will be demonstrated using an autostereoscopic display system (a stereoscopic display system that requires no device near the viewer's eyes) like the popular postcards that show a different scene depending on the viewing angle. The highest qual-

ity autostereoscopic displays require multiple stereo images, as described by Butterfield (1979). The artificial stereo algorithm on AOIPS can be used to generate many pseudo-perspective views. These images then can be used to produce an artificial autostereoscopic display.

The artificial stereo may be used as an important aid both in research, where repeated viewing continues to reveal more information, and in operational forecasting (e.g., nowcasting), where it is imperative that the maximum amount of information be assimilated in the least amount of time. Systems available now at the National Earth Satellite Service (NESS) in Washington and the National Severe Storms Forecast Center (NSSFC) in Kansas City are capable of producing this type of product in near-real time.

*Acknowledgments.* The authors thank John Taylor, who performed many of the data processing functions necessary to produce the artificial stereo images. Joe Woytek produced the smoothed infrared image used for the artificial stereo for Hurricane Allen. J. T. Young of the University of Wisconsin has been helpful for many years by sharing his ideas on image processing. Carl Kreitzberg provided the output from his mesoscale numerical model. Teresa Campbell kindly prepared the final manuscript.

#### References

- Bracken, P. A., J. T. Dalton, J. B. Billingsley, and J. Quann, 1977: Atmospheric and Oceanographic Information Processing System (AOIPS) system description. *NASA/GSFC X-933-77-148*, Goddard Space Flight Center, Greenbelt, Md., 110 pp.
- Butterfield, J. E., 1979: Autostereoscopy delivers what holography promised. Proceedings of the 23rd Annual SPIE Symposium, August 1979, Vol. 199, *Advances in Display Technology*. (Available from 3D VIDEO Corp., 10999 Riverside Dr., N. Hollywood, Calif. 91602.)
- desJardins, M., and A. F. Hasler, 1980: Stereographic displays of atmospheric model data. *Preprints, Seventh Annual Conference on Computer Graphics and Interactive Techniques (SIGGRAPH 80)*, (Seattle), Association for Computing Machines, Inc., New York, pp. 134-139.
- Hasler, A. F., 1981: Stereographic observations from geosynchronous satellites: An important new tool for the atmospheric sciences. *Bull. Am. Meteorol. Soc.*, **62**, 194-212.
- , and R. F. Adler, 1980: Cloud top structure of a tornadic thunderstorm from 3 min interval stereo satellite images compared with radar and other observations. *Preprints, 19th Conference on Radar Meteorology (Miami Beach)*, AMS, Boston, pp. 405-412.
- Kreitzberg, C. W., and D. J. Perkey, 1976: Release of potential instability: Part I. A sequential plume model within a hydrostatic primitive equation model. *J. Atmos. Sci.*, **33**, 456-475.
- , and —, 1977: Release of potential instability: Part II. The mechanism of convective/mesoscale interaction. *J. Atmos. Sci.*, **34**, 1569-1595.
- Moninger, W. R., and S. P. Nelson, 1980: Operational application of meteorological Doppler radar. Part VI: Postprocessing and display techniques. *Bull. Am. Meteorol. Soc.*, **61**, 1195-1203.
- Pichel, W., C. L. Bristor, and R. Brower, 1973: Artificial stereo: A technique for combining multi-channel satellite image data. *Bull. Am. Meteorol. Soc.*, **54**, 688-691.